3.16
Oceanic Plateaus

A. C. Kerr

Cardiff University, Wales, UK

3.16.1 INTRODUCTION

Although the existence of large continental flood basalt provinces has been known for some considerable time, e.g., Holmes (1918), the recognition that similar flood basalt provinces also exist below the oceans is relatively recent. In the early 1970s increasing amounts of evidence from seismic reflection and refraction studies revealed that the crust in several large portions of the ocean floor is significantly thicker than "normal" oceanic crust, which is 6–7 km thick. One of the first areas of such over-thickened crust to be identified was the Caribbean plate (Edgar *et al.*, 1971) which Donnelly (1973) proposed to be an "oceanic flood basalt province". The term oceanic plateau was coined by Kroenke (1974), and was prompted by the discovery of a large area of thickened crust (>30 km) in the western Pacific known as the Ontong Java plateau (OJP). As our knowledge of the ocean basins has improved over the last 25 years, many more oceanic plateaus have been identified (Figure 1). Coffin and Eldholm (1992) introduced the term "large igneous provinces" (LIPs) as a generic term encompassing oceanic plateaus, continental flood basalt provinces, and those provinces which form at the continent–ocean boundary (volcanic rifted margins).

LIPs are generally believed to be formed by decompression melting of upwelling hotter mantle, known as mantle plumes. Although ideas about hotpots and mantle plumes have been around for almost 40 years (Wilson, 1963), it is only in the past 15 years that LIPs have become the focus of major research. One of the main reasons for the increased research activity into LIPs is the realization that significant proportions of these LIPs erupted over a relatively short time, often less than 2–3 Myr (see review in Coffin, 1994).

This has important implications for mantle processes and source regions (Hart *et al.*, 1992; Stein and Hofmann, 1994), as well as environmental effects on the global biosphere (e.g., Caldeira and Rampino, 1990; Courtillot *et al.*, 1996; Kerr, 1998). Oceanic plateaus can also become accreted to continental margins, and it has been proposed that these plateaus have been significant contributors to the growth of continental crust (e.g., Abbott, 1996; Albarede, 1998).

The most recent major phase of oceanic plateau formation was in the Cretaceous when the Ontong Java, Manihiki, Hess Rise, and the Caribbean–Colombian plateaus formed in the Pacific, while in the Indian Ocean the Kerguelen plateau was developing. The areas, volume maximum thicknesses and ages of the larger of these plateaus are given in Table 1. The Ontong Java is the largest of the Cretaceous plateaus. It covers an area of 1.9×10^6 km^2, and has an estimated total volume of 4.4×10^7 km^3 (Eldholm and Coffin, 2000). Although early seismic refraction data suggested that the OJP was as thick as 43 km (Furomoto *et al.*, 1976), a more recent synthesis based on existing seismic and new gravity data (Gladczenko *et al.*, 1997) has indicated the average thickness to be ~32 km.

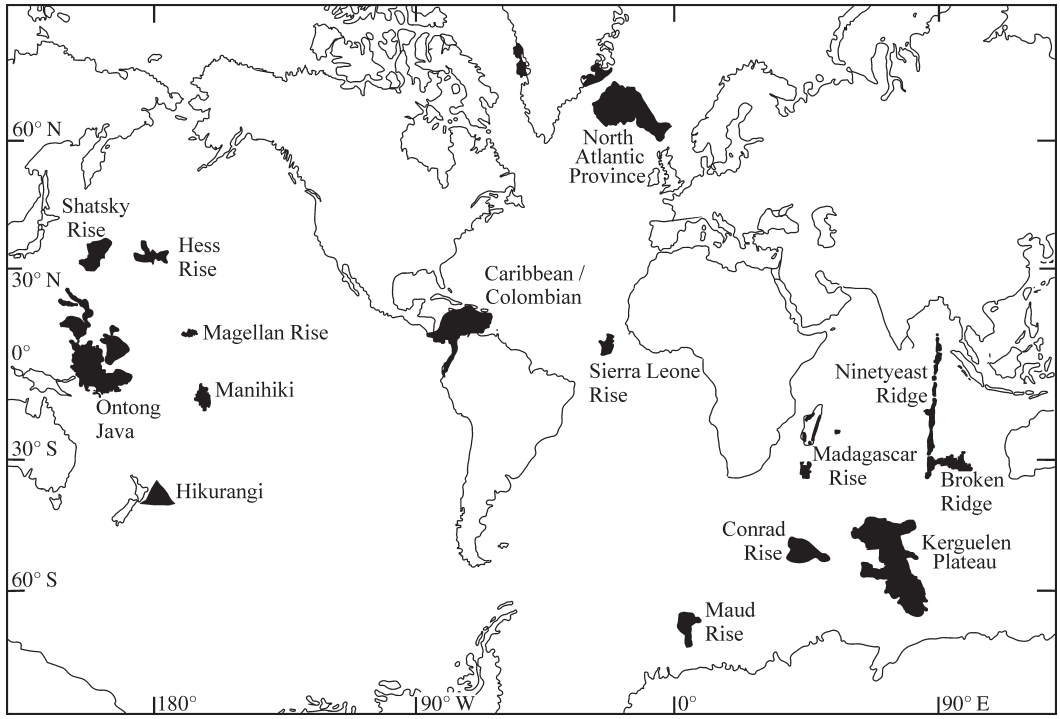

Figure 1 Map showing all major oceanic plateaus, and other large igneous provinces discussed in the text (after Saunders *et al.*, 1992).

Table 1 Ages and dimensions of Jurassic–Cretaceous oceanic plateaus.

Oceanic plateau	*Mean age* (Ma)	*Area* (10^6 km^2)	*Thickness range* (km)	*Volume* (10^6 km^3)
Hikurangi	early-mid Cretaceous	0.7	10–15	2.7
Shatsky Rise	147	0.2	10–28	2.5
Magellan Rise	145	0.5	10	1.8
Manihiki	123	0.8	>20	8.8
Ontong Java	121(90)	1.9	15–32	44.4
Hess Rise	99	0.8	>15	9.1
Caribbean	88	1.1	8–20	4.4
South Kerguelen	110	1.0	~22	6.0
Central Kerguelen/Broken Ridge	86	1.0	19–21	9.1
Sierra Leone Rise	~73	0.9	>10	2.5
Maud Rise	~>73	0.2	>10	1.2

After Eldholm and Coffin (2000).

3.16.2 FORMATION OF OCEANIC PLATEAUS

The production of large volumes ($>10^6$ km^3) of melt in a period as short as 2–3 Myr implies magma production rates up to 25% higher than those observed at present-day midocean ridges (Eldholm and Coffin, 2000), and is generally believed to necessitate a high flux of hotter-than-ambient asthenospheric mantle below these provinces (e.g., McKenzie and Bickle, 1988). Numerical and physical models show that this hotter mantle commonly takes the form of a mantle plume which ascends by thermal buoyancy through the overlying mantle (Loper, 1983; McKenzie and Bickle, 1988; Campbell *et al.*, 1989; Farnetani and Richards, 1995). Physical constraints demand that mantle plumes must ascend from a boundary layer within the Earth, either the core–mantle boundary (D'') or the 670 km discontinuity. Large ascending mantle plumes are, on average, 200 °C hotter than the ambient upper mantle (McKenzie and Bickle, 1988) and undergo decompression melting as they approach the base of the lithosphere. Physical modeling experiments by Griffiths and Campbell (1990) have shown that mantle plumes are likely to ascend through the mantle from their source boundary layer in the form of a large semi-spherical "head" fed from the source region by a narrower plume tail (Figure 2). Alternatively, numerical modeling by Farnetani and Richards (1995) suggested that plume heads starting in the mantle only rise about three plume head diameters before spreading out. In either case, as the plume approaches the base of the lithosphere, it spreads out over a broadly circular area (which can be as much as 1000 km in diameter) and undergoes adiabatic decompression, producing melt over most of the area covered by the flattened-out plume head (Campbell and Griffiths, 1990). The amount of melt produced is critically dependent on the thickness of the preexisting lithosphere, since the base of the rigid, nonconvecting lithosphere will act as a "lid" on the upwelling plume mantle and on the extent of decompression melting. Thus, a mantle plume ascending below thick continental lithosphere (>50 km) will produce a smaller thickness of melt than a plume which ascends beneath oceanic lithosphere (≤7 km) (Figure 3). Another significant factor in determining the amount of melt generated by a mantle plume is the temperature of the plume: generally the higher the temperature, the more melt will be produced (Figure 3).

The initial ^{40}Ar/^{39}Ar step-heating ages for LIPs support models of rapid formation and eruption, often in less than 2–3 Myr (Richards *et al.*, 1989). As more age data have become available, a wider age-range has emerged for some LIPs (e.g., the

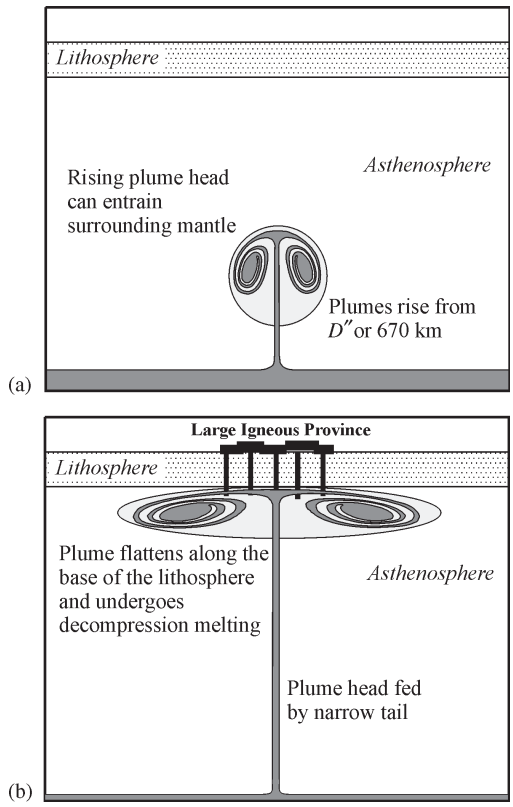

Figure 2 Cartoon to illustrate how mantle plumes are believed to (a) rise through the asthenosphere from either the 670 km discontinuity or D″ and (b) flatten along the base of the lithosphere and undergo decompression melting to produce a LIP (after Saunders *et al.*, 1992).

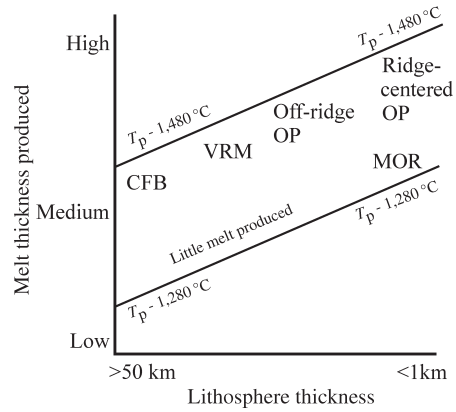

Figure 3 Schematic diagram showing how original lithospheric thickness and mantle potential temperature affect the amount of melt produced (melt thickness) and how these factors relate to continental flood basalts (CFB), volcanic rifted margins (VRM), off–ridge and ridge–centered oceanic plateaus (OP), and midocean ridges (MOR).

Caribbean plateau, 95–86 Ma: Kerr *et al.*, 1997a; Sinton *et al.*, 1998; Hauff *et al.*, 2000b). Nevertheless, it still appears that substantial proportions of these provinces were formed over geologically

short time periods (e.g., the Ontong Java plateau formed on two occasions: 122±3 and 90±4 Ma; Neal *et al.*, 1997).

Theoretically, oceanic plateaus can form anywhere in the ocean basins; however, most oceanic plateaus appear to have formed at or near midocean ridges (e.g., Kerguelen, Manihiki and Ontong Java), i.e., regions that are conducive to voluminous decompression melting (Eldholm and Coffin, 2000). At first glance, it appears somewhat coincidental that plumes of deep mantle origin reach the base of the lithosphere at a midocean ridge. However, as pointed out by Saunders *et al.* (1996), a likely explanation for this observation is that mantle plumes can "capture" oceanic spreading centers (cf. present-day Iceland).

3.16.3 PRESERVATION OF OCEANIC PLATEAUS

The oldest *in situ* oceanic crust is Jurassic in age (Pringle, 1992), because within 200 Myr of its formation at a midocean ridge, the oceanic crust was recycled back into the asthenosphere. Although many of the Cretaceous and late Jurassic oceanic plateaus still form part of the ocean basins, the preservation potential of oceanic plateaus older than Jurassic is low. Fortunately, however, oceanic plateaus are much more buoyant than oceanic crust of "normal" thickness formed at a midocean ridge (e.g., Cloos, 1993). This excess buoyancy is primarily due to the greater crustal thickness of oceanic plateaus if the plateaus are relatively young; residual heat from their formation can also contribute to their buoyancy. Recent measurements of upper mantle shear wave splitting and shear wave velocity structure (Klosko *et al.*, 2001) reveal that the Ontong Java plateau is underlain by a 300 km thick, long-lived, rheologically strong and chemically depleted root. Klosko *et al.* (2001) propose that this root represents the residue from mantle melting and that its consequent lower density contributes significantly to the buoyancy of both the Ontong Java and other oceanic plateaus. The net result of this excess buoyancy is that oceanic plateaus, in contrast to normal oceanic crust, are much less easily subducted (Ben-Avraham *et al.*, 1981; Cloos, 1993; Kimura and Ludden, 1995). Instead of being completely recycled back into the mantle, their upper layers can be "peeled off" (Kimura and Ludden, 1995) and accreted on to the margin of the subduction zone. This plateau accretion can occur either at an Andean-type continental margin, or an island arc.

Although many of the in situ Cretaceous oceanic plateaus have been drilled by the Deep Sea Drilling (DSDP) and Ocean Drilling Programs (ODP), the insight that these drill holes can provide is relatively limited compared to the accreted oceanic plateau sections. For example, the Ontong Java plateau collided with the westward-dipping Solomon Islands subduction zone at 10–20 Ma, resulting in a reversal in the polarity of subduction from west to east, and the uplift and exposure of the deeper sections of the plateau on the Solomon Islands (Neal *et al.*, 1997; Petterson *et al.*, 1999). A second example is the Caribbean–Colombian oceanic plateau, which formed in the Pacific at ~90 Ma (Sinton *et al.*, 1998; Hauff *et al.*, 2000a). Within 10 Myr the eastward-moving Farallon plate had brought the southern portion of the plateau into collision with continental northwestern South America, resulting in the accretion of slices of the plateau on to the continental margin (Kerr *et al.*, 1997b). This accretion was accompanied by back-stepping of the subduction zone west of the accreted plateau slices. Shortly after its formation the northern portion of the plateau began to move into the proto-Caribbean seaway between North and South America (Burke, 1988; Kerr *et al.*, 1999; White *et al.*, 1999). In doing so the plateau encountered the eastward-dipping "Great Arc of the Caribbean". Unable to subduct, the thick plateau clogged the subduction zone, resulting in a reversal in the polarity of subduction from east to west. This reversal in subduction polarity in conjunction with a back-stepping of subduction behind the advancing plateau (Burke, 1988), effectively isolated the Caribbean as a separate plate. Over the past ~80 Ma the northern portion of the Caribbean plateau has moved into the gap between North and South America and has been uplifted and subaerially exposed around its margins (Figure 4), thus making it available for detailed study. It is in ways such as these that remnants of these thick, buoyant oceanic plateaus can be preserved and incorporated into the continental crust. The identification of these older preserved plateaus within the geological record will be explored in a later section.

3.16.4 GEOCHEMISTRY OF CRETACEOUS OCEANIC PLATEAUS

3.16.4.1 General Chemical Characteristics

Table 2 shows representative analyses of *in situ* and accreted portions of Cretaceous oceanic plateaus. Cretaceous oceanic plateaus are predominantly basaltic (<10 wt.% MgO) in composition (Figure 5), although more-MgO-rich lava flows are found in the Caribbean–Colombian oceanic plateau (CCOP). Typically, oceanic plateaus possess generally low levels of compatible elements (i.e., Ni < 300 ppm and Cr < 1,000 ppm; see Figure 6). In terms of incompatible trace elements the majority of oceanic plateau lavas and intrusive sheets possess relatively flat rare earth

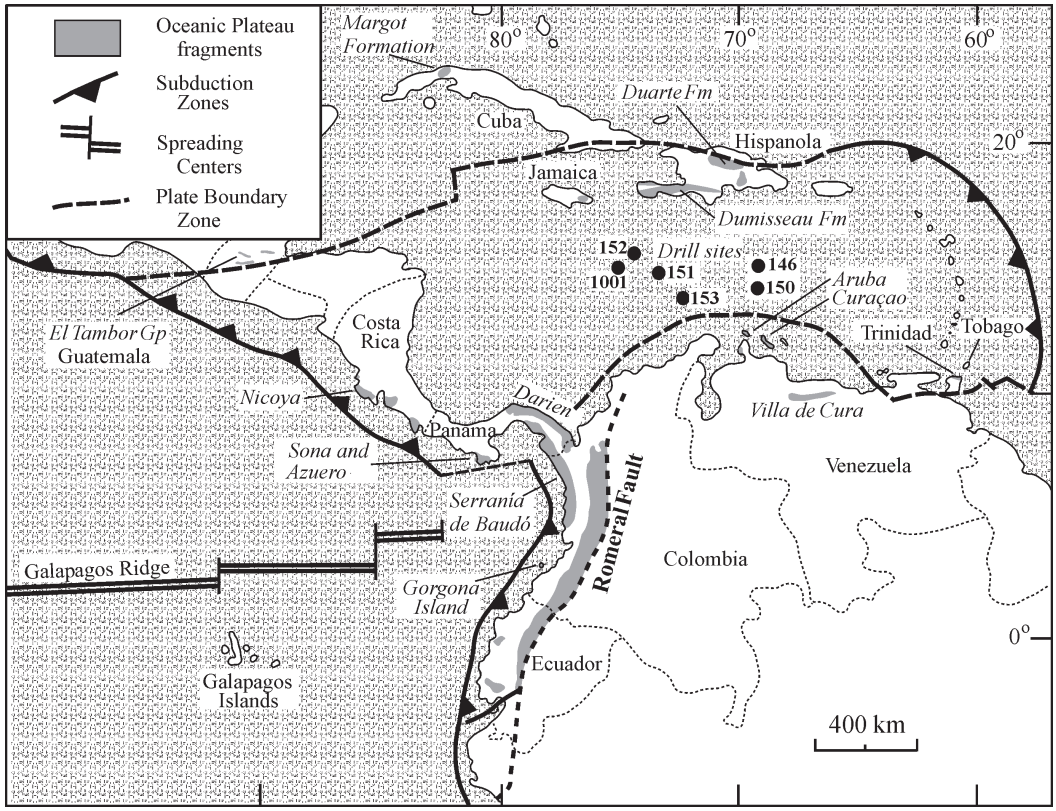

Figure 4 Map to show the main accreted outcrops of the Caribbean–Colombian oceanic plateau along with the locations of DSDP/ODP drill holes which penetrated the thickened crust of the Caribbean plate.

primitive mantle-normalized patterns with abundances varying between 5 and 10 times primitive mantle values (Figure 7).

The radiogenic isotope compositions of oceanic plateaus have been well characterized: initial εNd values for oceanic plateaus generally range from +6.0 to +9.0, whereas initial $^{87}Sr/^{86}Sr$ ratios fall mostly between 0.703 and 0.704 (Figure 8), i.e., the $^{87}Sr/^{86}Sr$ and $\varepsilon >$ Nd values are generally less depleted in terms of their radiogenic isotopes than "normal" (N)-MORB as typified by MORB from the East Pacific Rise (Figure 8(a)). Elevated initial $^{87}Sr/^{86}Sr$ ratios (>0.7040) are most likely due to secondary alteration by hydrothermal fluids. It is noteworthy that the high-MgO rocks generally possess more extreme $(\varepsilon Nd)_i$ values than the basalts (Figure 8(a)). Figure 8(b), a plot of $^{207}Pb/^{204}Pb$ against $^{206}Pb/^{204}Pb$, reveals that most oceanic plateau rocks range between 18.5 and 19.5 $^{206}Pb/^{204}Pb$ and between 15.525 and 15.625 $^{207}Pb/^{204}Pb$. An interesting feature of Figure 8(b) is that many of the basalts lie on a trend between the proposed mantle components of HIMU and DMM (Zindler and Hart, 1986) while the high-MgO lavas form a trend between DMM and the enriched mantle component EM2. Zindler and Hart (1986) proposed four mantle components: depleted MORB mantle (DMM), two types of enriched mantle EM1 and EM2, and HIMU, so-called because it has a high $^{238}U/^{204}Pb$ ratio, or μ value.

In recent years our knowledge of the radiogenic isotope systematics of oceanic plateaus has been augmented by the analysis of Hf and Os isotopes. Although data for the Kerguelen and Ontong Java plateaus are still relatively sparse, more data exist for the CCOP. Initial εHf values for the CCOP and OJP range from 10 to 18 (Figure 9(a)). The CCOP samples form a trend between MORB source mantle and the HIMU component, while the OJP samples possess lower initial εNd values at equivalent εHf than the CCOP and appear to form a trend towards EM2. The much lower εHf and εNd for the Kerguelen plateau (Figure 9(a)) will be discussed in Section 3.16.5.2. Initial γOs for high-MgO rocks from the CCOP range from 0 to +18, whereas the basalts range from −7 to +10 (Figure 9(b)). How representative these ranges are for γOs, requires the acquisition of more data from other oceanic plateaus.

3.16.4.2 Mantle Plume Source Regions of Oceanic Plateaus

Since the pioneering study of Hoffman and White, it has become widely accepted that one of

Table 2 Representative analyses of Cretaceous oceanic plateau lavas.

Plateau	*Location*	*Sample*	*Data sources*	*Zr*	*Nb*	*Mo*	*Hf*	*Pb*	*Ta*	*Th*	*U*	$^{87}Sr/^{86}Sri$	*εNdi*	$^{206}Pb/^{204}Pb$	$^{207}Pb/^{204}Pb$	$^{208}Pb/^{204}Pb$
Kerguelen	ODP site 747	16-5,103-6	1	50.90	1.21	17.23	10.62	0.16	7.47	9.59	1.88	2.00	0.16	101.22	3.63	
Kerguelen	ODP site 748	79-6,90-4	1	49.24	2.74	17.50	8.77	0.09	7.54	6.71	4.72	0.56	1.12	98.99	7.14	
Kerguelen	ODP site 749	15-5,125-7	1	52.73	1.52	15.18	11.95	0.17	7.22	8.31	3.42	0.54	0.18	101.22	1.35	
Kerguelen	ODP site 750	17-3,23-26	1	49.21	1.17	15.77	14.62	0.18	8.36	9.01	1.99	0.19	0.11	100.61	4.31	
Kerguelen	ODP site 738	34-1,88-92	2	52.17	1.73	15.44	10.82	0.18	5.51	9.17	2.98	1.95	0.21	100.16	0.58	
Ontong Java	ODP site 807	75-4,46-48	3	48.75	1.62	14.16	13.43	0.21	6.74	12.13	2.38	0.13	0.14	99.69	0.45	
Ontong Java	ODP site 807	88-3,76-79	3	49.74	1.13	14.27	13.44	0.22	7.43	12.00	2.06	0.28	0.09	100.66	−0.24	
Ontong Java	Santa Isabel	I96	4	49.28	1.31	14.20	12.44	0.16	8.03	12.50	1.89	0.15	0.10	100.06	1.61	
Ontong Java	Maliata	SG1	5	50.38	1.65	13.54	14.01	0.19	7.30	11.64	2.32	0.15	0.14	101.32	0.30	6.0
Ontong Java	Maliata	ML407	5	49.67	1.35	13.64	13.47	0.19	7.45	11.38	3.08	0.26	0.13	100.62	2.14	5.0
CCOP	Gorgona	GOR160	6	45.13	0.64	11.78	12.52	0.18	18.25	10.10	1.30	0.06	0.05	100.01		
CCOP	Gorgona	GOR117	6	50.40	0.77	13.81	12.62	0.23	8.65	12.39	2.43	0.02	0.06	101.38		
CCOP	Gorgona	GOR94-35	7	46.58	0.37	10.57	11.41	0.17	21.96	8.42	0.55	0.19	0.03	100.25	3.26	
CCOP	Colombia	SDB18	8	50.63	1.47	14.19	13.34	0.23	6.77	10.94	2.89	0.15	0.12	100.72	1.57	
CCOP	Colombia	VIJ1	8	51.45	2.02	12.85	15.20	0.19	5.78	9.57	2.29	0.07	0.17	99.59	0.90	
CCOP	Colombia	COL472	9	48.81	0.89	12.86	10.66	0.17	11.55	11.61	2.91	0.08	0.09	99.64	3.03	
CCOP	Curaçao	CUR14	10	46.42	0.57	9.53	11.06	0.17	22.86	8.20	0.90	0.02	0.05	99.79	2.23	
CCOP	Curaçao	CUR20	10	52.13	0.78	12.85	9.80	0.20	8.60	14.30	1.43	0.03	0.06	100.18	1.41	
CCOP	DSDP site 150	11-2, 63-67	11	49.46	1.27	16.60	10.30	0.10	8.58	9.87	2.60	0.13	0.10	99.02		
CCOP	Ecuador	EQ1	12	48.88	1.23	14.39	12.75	0.20	8.96	10.81	1.89	0.72	0.18	100.01	4.45	

				Rb	Cs	Sr	Ba	Sc	V	Cr	Ni	Cu	Zn	Ga	La	Ce
Kerguelen	ODP site 747	16-5,103-6	1	18.5	<0.8	234	229	33.8	201	401	72		66	22.0	12.30	25.50
Kerguelen	ODP site 748	79-6,90-4	1	7.8	2.81	1131	1661	18.7	170	166	182		79	18.7	105.00	224.00
Kerguelen	ODP site 749	15-5,125-7	1	12.3	<0.5	214	114	34.5	271	260	30		115	22.7	6.80	16.10
Kerguelen	ODP site 750	17-3,23-26	1	9.0	<0.9	193	30	38.9	269	193	120		93	19.8	4.00	8.90
Kerguelen	ODP site 738	34-1,88-92	2	37.4		273	336	36.9	267	95	28		102	20.7	17.10	39.30
Ontong Java	ODP site 807	75-4,46-48	3	1.0		174		45.9	313	162	99				6.15	14.59
Ontong Java	ODP site 807	88-3,76-79	3	10.0		107		52.3	349	163	87				2.96	8.07
Ontong Java	Santa Isabel	I96	4	2.0		115	37	50.0	341	238	122				3.40	9.90
Ontong Java	Maliata	SG1	5	1.3	0.01	108	28	41.0	392	56	61	124	93	17.0	4.75	12.60
Ontong Java	Maliata	ML407	5	1.8	0.01	100	23	40.0	295	61	62	229	57	17.0	3.86	10.60
CCOP	Gorgona	GOR160	6	1.0		64	8	28.3	227	1373	723			13.2	0.65	2.17
CCOP	Gorgona	GOR117	6	0.3		107	21	41.1	371	194	112			15.7	1.02	2.99
CCOP	Gorgona	GOR94-35	7	4.2		34	20	27.3	166	82	968	2030	56	10.8	0.22	0.57
CCOP	Colombia	SDB18	8	2.5		156	37	42.2	331	208	97			19.1	3.80	9.80
CCOP	Colombia	VIJ1	8	0.4		89	27	44.4	531	63	58	133	124	20.2	6.05	16.55
CCOP	Colombia	COL472	9	1.9		398	85	30.8	334	1393	264	125	70	14.3	2.42	6.33

CCOP	Curaçao	CUR14	10	1.7		46	6	29.7	186	2017	1032	75	70	9.1	1.20	4.20
CCOP	Curaçao	CUR20	10	0.4		69	11	43.3	258	552	178	102	66	12.2	2.84	7.59
CCOP	DSDP site 150	11-2, 63-67	11	3.2		117	16		335	373	127	150	85	17.0	3.16	8.55
CCOP	Ecuador	EQ1	12	5.2		111	15	61.5	353	285	101				3.50	9.63

				Pr	Nd	Sm	Eu	Gd	Tb	Dy	Ho	Er	Tm	Yb	Lu	Y
Kerguelen	ODP site 747	16-5,103-6	1		13.50	3.50	1.03	0.00	0.65					1.89	0.28	23.2
Kerguelen	ODP site 748	79-6,90-4	1		103.00	14.20	3.31	8.90	1.25					1.80	0.26	27.7
Kerguelen	ODP site 749	15-5,125-7	1		11.90	3.64	1.24		0.69					2.71	0.39	29.3
Kerguelen	ODP site 750	17-3,23-26	1		6.30	2.32	0.84	3.00	0.58					2.57	0.34	24.6
Kerguelen	ODP site 738	34-1,88-92	2		21.20	5.28	1.73		0.94					2.87	0.44	28.8
Ontong Java	ODP site 807	75-4,46-48	3		11.65	3.39	1.31	4.51	0.81					2.71	0.42	30.0
Ontong Java	ODP site 807	88-3,76-79	3		6.50	2.30	0.93	3.39	0.70					2.40	0.38	24.0
Ontong Java	Santa Isabel	I96	4	1.56	7.84	2.77	1.02	3.50	0.63	4.20	0.91	2.64	0.37	2.30	0.35	22.0
Ontong Java	Maliata	SG1	5	1.98	4.61	1.69	1.13	4.14	0.73	4.56	1.00	2.90	0.41	2.83	0.43	25.0
Ontong Java	Maliata	ML407	5	1.70	5.67	2.11	0.94	3.54	0.68	4.22	0.92	2.57	0.36	2.47	0.37	23.0
CCOP	Gorgona	GOR160	6	0.46	2.86	1.25	0.48	1.58	0.29	2.10		1.43	0.22	1.30	0.21	13.8
CCOP	Gorgona	GOR117	6	0.60	3.53	1.74	0.63	2.07	0.41	3.13		2.18	0.37	2.20	0.32	22.8
CCOP	Gorgona	GOR94-35	7	0.13	0.90	0.65	0.34	1.50	0.30	2.18	0.48	1.44	0.23	1.42	0.21	15.3
CCOP	Colombia	SDB18	8		9.30	2.85	1.11	2.94	0.80					2.75	0.43	29.4
CCOP	Colombia	VIJ1	8		12.0	3.97	1.47	4.76	0.93					4.25	0.63	41.7
CCOP	Colombia	COL472	9	0.92	5.58	1.76	0.74	2.67		2.92	0.58	1.44		1.36	0.21	19.0
CCOP	Curaçao	CUR14	10		3.16		0.38							0.50		11.5
CCOP	Curaçao	CUR20	10	0.79	4.80	1.39	0.55	1.87		2.11	0.45	1.38		1.36	0.21	15.8
CCOP	DSDP site 150	11-2, 63-67	11	1.36	6.94	2.32	0.89	2.87	0.52	3.36	0.69	1.89	0.28	1.82	0.26	21.0
CCOP	Ecuador	EQ1	12	1.56	8.11	2.57	0.96	3.46	0.66	4.40	0.90	2.60	0.39	2.53	0.38	22.3

				Zr	Nb	Mo	Hf	Pb	Ta	Th	U	$^{87}Sr/^{86}Sri$	εNdi	$^{206}Pb/^{204}Pb$	$^{207}Pb/^{204}Pb$	$^{208}Pb/^{204}Pb$
Kerguelen	ODP site 747	16-5,103-6	1	97	7.00		2.34		0.46	0.20	0.000	0.705783	−4.0	17.65	15.51	38.16
Kerguelen	ODP site 748	79-6,90-4	1	599	121.90		12.40	8.00	9.08	13.20	2.200	0.705319	−3.3	18.19	15.64	38.38
Kerguelen	ODP site 749	15-5,125-7	1	91	5.80		2.16	1.63	0.40	1.80	0.148	0.704260	1.8	18.03	15.55	38.16
Kerguelen	ODP site 750	17-3,23-26	1	47	3.33		1.16	0.82	0.19	1.40	0.048	0.706165	1.4	17.53	15.49	38.01
Kerguelen	ODP site 738	34-1,88-92	2	166	8.90		3.89		0.54	2.27		0.709730	−8.2	17.82	15.75	39.01
Ontong Java	ODP site 807	75-4,46-48	3	98	5.70		2.64		0.34	0.56		0.704330	5.0	18.40	15.53	38.38
Ontong Java	ODP site 807	88-3,76-79	3	64	3.32		1.74		0.20	0.34		0.703560	5.9	18.67	15.55	38.54
Ontong Java	Santa Isabel	I96	4	65	4.30			0.23		0.27	0.120	0.703690	5.4	18.64	15.54	38.60
Ontong Java	Maliata	SG1	5	81	4.90	0.59	2.50	0.17	0.35	0.28	0.097	0.704040	3.9	17.85	15.47	37.91
Ontong Java	Maliata	ML407	5	83	5.00	0.36	2.63	0.15	0.25	0.16	0.047	0.704130	5.7	18.32	15.51	38.23
CCOP	Gorgona	GOR160	6	29	0.48		1.00	1.30		0.02	0.011	0.703041	9.5	18.32	15.50	37.82

(continued)

Table 2 (continued).

Plateau	*Location*	*Sample*	*Data sources*	*Zr*	*Nb*	*Mo*	*Hf*	*Pb*	*Ta*	*Th*	*U*	$^{87}Sr/^{86}Sri$	εNdi	$^{206}Pb/^{204}Pb$	$^{207}Pb/^{204}Pb$	$^{208}Pb/^{204}Pb$
CCOP	Gorgona	GOR117	6	39	0.87		1.05	12.10		0.08	0.034	0.703283	8.6	18.86	15.58	38.56
CCOP	Gorgona	GOR94-35	7	13	0.80					1.20		0.704767	9.4	18.68	15.54	38.19
CCOP	Colombia	SDB18	8	70	4.29		2.05		0.30	0.30		0.703380	8.5	18.87	15.54	38.46
CCOP	Colombia	VIJ1	8	119	8.00		3.14		0.48	0.62	0.210	0.703207	8.1	19.22	15.58	38.91
CCOP	Colombia	COL472	9	40	2.16			2.37				0.513197	11.0	19.33	15.58	38.86
CCOP	Curaçao	CUR14	10	30	2.50			1.20		0.10		0.702961	6.6	19.31	15.59	38.90
CCOP	Curaçao	CUR20	10	40	3.40			1.00		0.90		0.703215	7.0	19.08	15.55	38.82
CCOP	DSDP site 150	11-2, 63-67	11	68	11.00		1.92	0.23	0.23	0.26	0.094	0.703546	7.2	19.07	15.60	38.70
CCOP	Ecuador	EQ1	12	60	4.16		1.89	0.14	0.58	0.25	0.080	0.703200	10.1	18.16	15.53	37.84

Sources: 1 Salters *et al.* (1992), 2 Mahoney *et al.* (1995), 3 Mahoney *et al.* (1993a), 4 Tejada *et al.* (1996), 5 Tejada *et al.* (2002), 6 Aitken and Echeverría (1984), Dupré and Echeverría (1984), Jochum *et al.* (1991), 7 AC Kerr unpublished data, 8 Kerr *et al.* (1997), Hauff *et al.* (2000b), 9 Kerr *et al.* (2002), 10 Kerr *et al.* (1996b), 11 Hauff *et al.* (2000b), 12 Reynaud *et al.* (1999).

the principal contributors to the source regions of deep mantle plumes are subducted oceanic slabs and their sediments which descended through the asthenospheric mantle and ponded at either the 670 km discontinuity or the core–mantle boundary (D″). Zindler and Hart (1986) identified three main mantle plume components: HIMU (proposed as being derived from subducted oceanic crust); and two enriched components, EM1 and EM2. In addition, the upper asthenosphere was proposed as consisting of depleted MORB mantle (DMM).

More recently, it has been shown that depleted signatures found in some LIPs represent a component which, rather than being due to entrainment of depleted upper mantle material (DMM), is derived from depth, and so is an integral part the plume itself (Kerr *et al.*, 1995a,b; Fitton *et al.*, 1997; Kempton *et al.*, 2000). Kerr *et al.* (1995a,b) and Walker *et al.* (1999) proposed that this depleted plume component was ultimately derived from subducted oceanic lithosphere, unlike HIMU, which has its source in more-enriched upper oceanic crust.

Evidence for recycled oceanic crust and lithosphere in the mantle plume source regions of oceanic plateaus has been presented by several authors (e.g., Walker *et al.*, 1999; Hauff *et al.*, 2000a), and mixing trends between a depleted component and HIMU are clearly seen on most of the radiogenic isotope plots (Figures 8 and 9).

3.16.4.3 Caribbean–Colombian Oceanic Plateau (~90 Ma)

The Caribbean–Colombian Oceanic Plateau (CCOP) is exposed around the margins of the Caribbean and along the northwestern continental margin of South America (Figure 4). The thickened nature of the bulk of the Caribbean plate (8–20 km; Edgar *et al.*, 1971; Mauffret and Leroy, 1997) testifies to its origin as an oceanic plateau. The plateau has been drilled by DSDP Leg 15 and ODP Leg 165 (Figure 4; Bence *et al.*, 1975; Sinton *et al.*, 2000). The accreted plateau material in Colombia, Ecuador, Costa Rica and Hispaniola consists of fault-bounded slices of basaltic, and occasionally picritic lavas and sills with relatively few intercalated sediments and ash layers (Kerr *et al.*, 1997a). Although they preserve layered and isotropic gabbros and ultramafic rocks, unlike accreted ophiolites generated at spreading centers, these accreted sequences of oceanic plateau do not possess sheeted dyke complexes (Kerr *et al.*, 1998).

Several other exposures are worthy of special mention: firstly, the 5 km thick section on the island of Curaçao, 70 km north of the coast of Venezuela (Figure 4). The sequence consists of

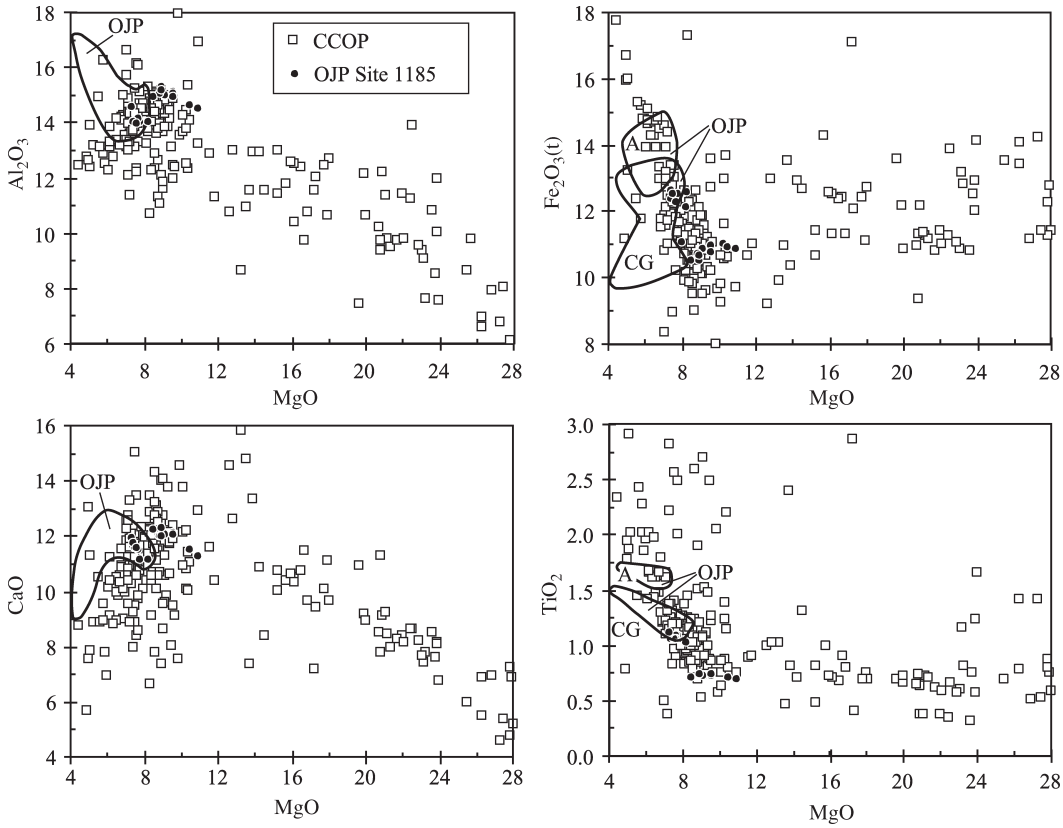

Figure 5 Plots of major elements (wt.%) against wt.% MgO for lavas from throughout the CCOP. All lavas with >18 wt.% MgO contain accumulated olivine. Data sources: Colombia—Kerr *et al.* (1997a), Gorgona—Echeverría (1980), Kerr *et al.* (1996a), Arndt *et al.* (1997), Costa Rica—Hauff *et al.* (2000b), Curaçao—Kerr *et al.* (1996b). Circled fields are from the Ontong Java plateau (Mahoney *et al.*, 1993a,b). Where the A and CG types differ markedly in composition they are plotted as separate fields, otherwise the OJP is plotted as a single field. OJP Site 1185 unpublished data were kindly provided by Godfrey Fitton.

pillowed picrites (MgO >12 wt.%) low in the succession that gradually give way to more basaltic pillow lavas nearer the top. These pillow lavas are intercalated with hyaloclastite horizons and intrusive sheets (Klaver, 1987; Kerr *et al.*, 1996b). The second noteworthy locality is the island of Gorgona, 50 km off the western coast of Colombia (Figure 4). This small island (2.5 × 8 km) is the site of the youngest komatiites (MgO-rich lava flows: >15 wt.%), which possess platy and blade-shaped olivines, giving the rocks a characteristic "spinifex" texture (Echeverría, 1980; Kerr *et al.*, 1996a). Komatiites are relatively common in the pre-Cambrian, however, the only known Phanerozoic komatiites occur as part of the CCOP on Gorgona Island. The formation of these Cretaceous komatiites in the CCOP has led to the suggestion that pre-Cambrian komatiites formed in ancient oceanic plateaus (Storey *et al.*, 1991).

The lavas of the CCOP are classified as tholeiitic. The most magnesian lavas found in the province contain up to 28 wt.% MgO (Figure 5). However, as shown by Kerr *et al.* (1996b), it is likely that these lavas contain substantial accumulated olivine, and so the whole rock compositions of these high-MgO rocks cannot represent those of parental mantle melts. Estimates of the MgO content of the parental melts for various parts of the province vary from 18 wt.% MgO to about 12 wt.% MgO (Kerr *et al.*, 1996a,b; Revillon *et al.*, 1999). Although picritic lavas are more common than in other Cretaceous oceanic plateaus, basalts are by far the most common rock type preserved in the CCOP. The vast majority of samples contain between 6 and 10 wt.% MgO (Figure 5). Al_2O_3 contents broadly increase with decreasing MgO, reflecting the importance of the addition and removal of olivine during the petrogenetic history of the CCOP lavas. CaO increases with decreasing MgO until MgO reaches 8–10 wt.% beyond which the CCOP lavas display a scattered but discernible downward trend. $Fe_2O_3(t)$ and TiO_2 display broadly horizontal trends until about 8–10 wt.% MgO, below which both increase markedly. These trends can be modeled by the initial fractional crystallization or accumulation of

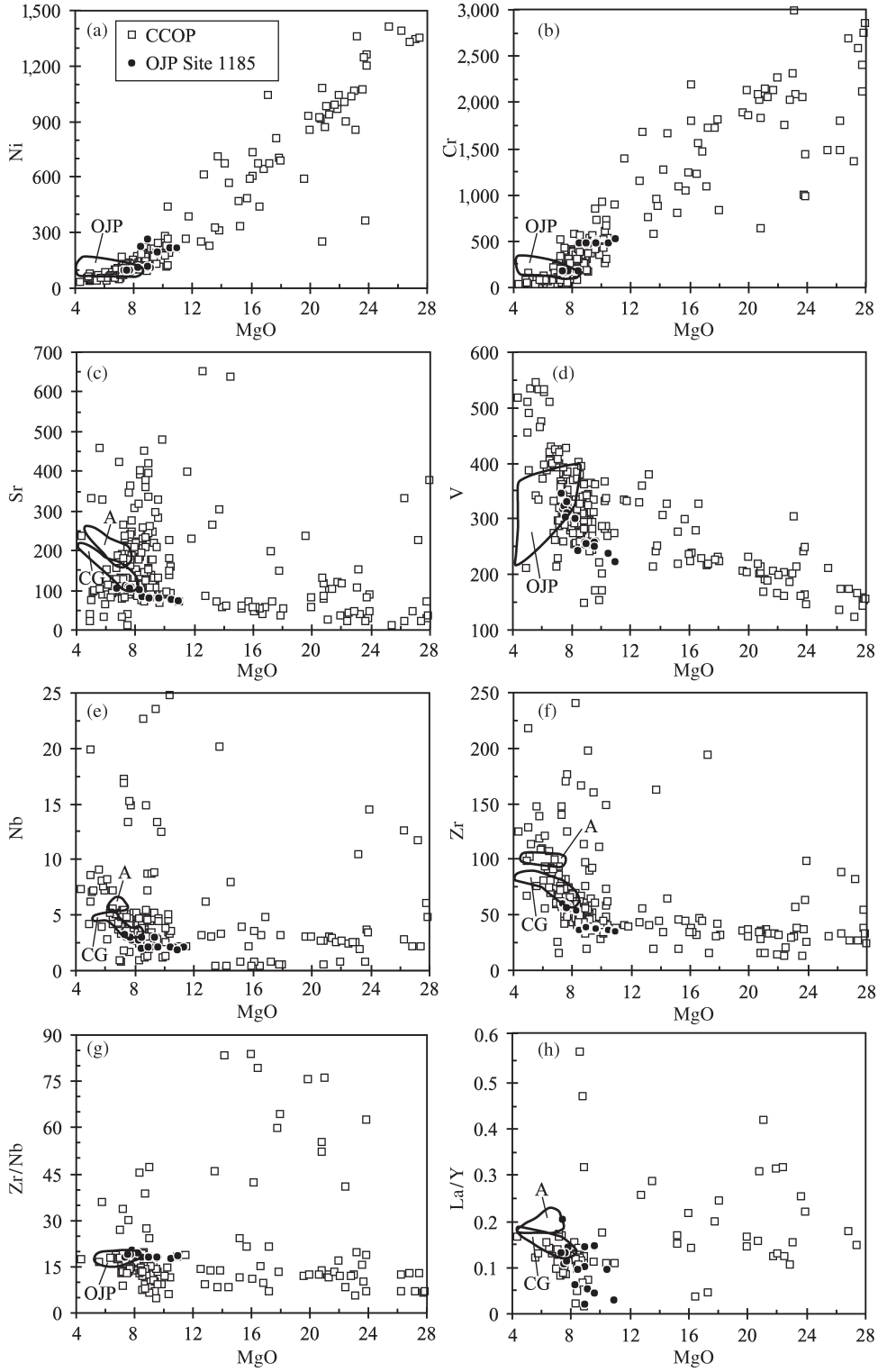

Figure 6 Plots of trace elements (ppm) and ratios of trace elements against wt.% MgO for lavas from the CCOP. The OJP is plotted as a single field except where the A and CG types differ markedly in composition. Data sources are as for Figure 5.

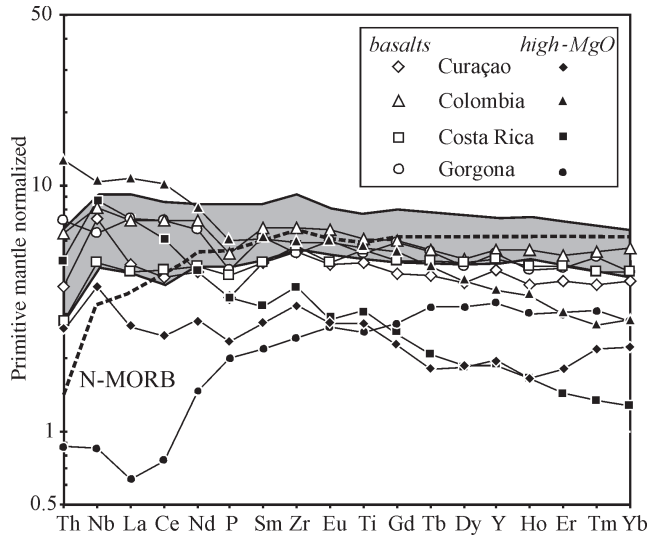

Figure 7 Primitive mantle normalized multi-element plot showing the average composition of high-MgO lavas (komatiites and picrites) and basalts from various parts of the CCOP, plotted along with average N-MORB values (dashed line) and a compositional field for the OJP. Data sources are as for Figure 5. Primitive mantle normalizing values and N-MORB from Sun and McDonough (1989).

olivine (plus minor Cr-spinel) followed by the commencement of crystallization of plagioclase and clinopyroxene between 8 wt.% MgO and 10 wt.% MgO (Kerr *et al.*, 1996b).

Trace element data (Figure 6) also support the proposed fractional crystallization model: Ni and Cr contents fall with decreasing MgO contents, and Sr, although commonly disturbed by sub-solidus alteration processes, is generally reduced below 10 wt.% MgO. Despite some scatter, the content of incompatible trace elements, e.g., Nb and Zr, generally increases with decreasing MgO contents (Figure 6). Ratios of highly incompatible trace elements are not normally affected by moderate degrees of fractional crystallization or mantle melting, and they therefore have the potential to reveal heterogeneities in the mantle source region of the plateau. These ratios are plotted against MgO in Figure 6(g)–(h). One of the most interesting aspects of the trace element data for the CCOP is that the basaltic lavas possess a narrower range of incompatible trace element ratios than the picrites. For instance, well over 80% of the basaltic samples (<12 wt.% MgO) from the CCOP possess La/Y ratios between 0.05 and 0.2 and Zr/Nb ratios between 7 and 20 (Figure 6(g)–(h)). In contrast, the picritic and komatiitic lavas possess much more variable ratios of incompatible trace elements, with La/Y ranging from 0.05 to 0.45 and Zr/Nb from 5 to 85. This is also shown on primitive mantle normalized multielement plots, where it can be seen that the CCOP basalts possess broadly flat patterns whereas the high-MgO picrites and komatiites are generally much more variable, with some being more depleted, and some more enriched than the basalts, particularly for the most highly incompatible trace elements such as Th, Nb, La, Ce & Nd (Figure 7).

The heterogeneity of the high-MgO rocks is also reflected in the radiogenic isotope ratios, particularly εNd (Figures 8 and 9). Virtually all the analyzed basalts from the CCOP possess initial εNd ranging from +6 to +9, whereas the high MgO lavas generally fall outside this range (εNd $>+9$ and $<+6$; Figure 8). Elevated initial $^{87}Sr/^{86}Sr$ ratios found in several parts of the province have been attributed either to contamination with altered oceanic crust (Curaçao: Kerr *et al.*, 1996b) or to secondary alteration (Gorgona: Revillon *et al.*, 1999).

The wide range of isotopic data for the CCOP reveals that the enriched and depleted lavas are not simply formed by variable melting of a homogeneous source region, but rather reflect melting of long-term depleted and enriched components from a markedly heterogeneous plume source region. (Kerr *et al.*, 1996a, 2002; Arndt *et al.*, 1997; Hauff *et al.*, 2000a; Thompson *et al.*, 2004).

The greater heterogeneity of the high MgO rocks in comparison to the basalts, has been interpreted to reflect the formation of these lower MgO magmas through mixing and fractional crystallisation of the high-MgO magmas in large magma chambers. The heterogeneous high-MgO rocks thus represent magmas that passed relatively quickly through the lithosphere without being trapped in magma chambers (Kerr *et al.*, 1998). The extent of partial melting required to produce

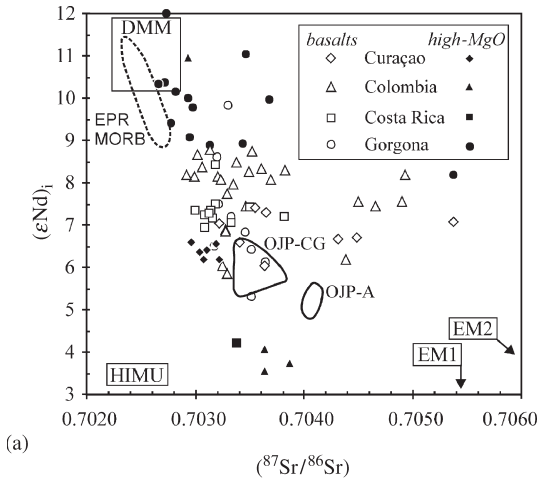

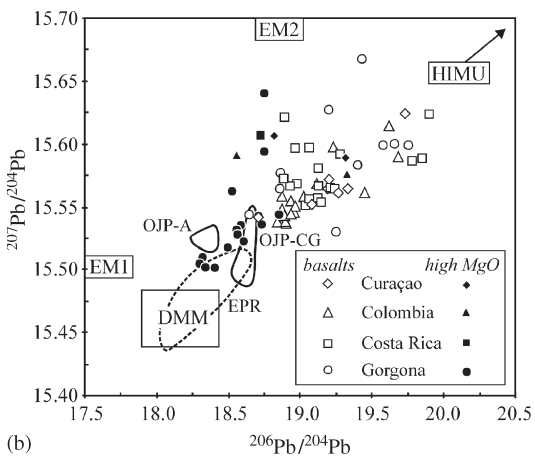

Figure 8 Plot of (a) initial εNd against $^{87}Sr/^{86}Sr$ for high-MgO lavas and basalts from the CCOP and (b) $^{207}Pb/^{204}Pb$ against $^{206}Pb/^{204}Pb$. Shown on both diagrams are fields for the OJP- A and CG types (Mahoney *et al.*, 1993a,b) and East Pacific Rise (EPR) MORB (Mahoney *et al.*, 1995). Other data sources are as for Figure 5. Mantle end-member compositions are from Zindler and Hart (1986).

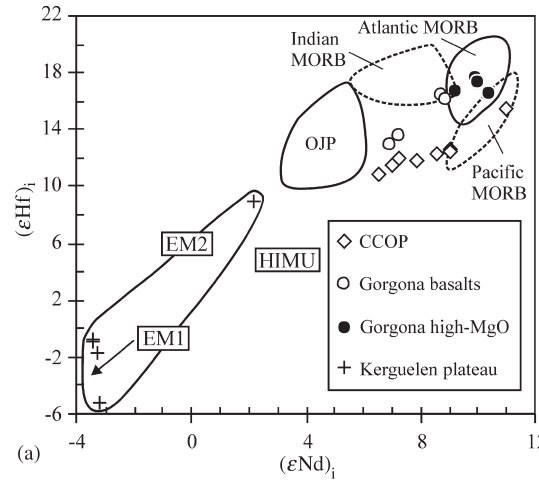

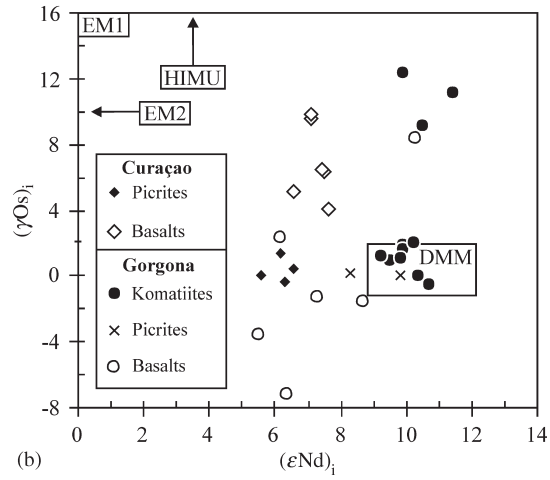

Figure 9 Plots of (a) initial εHf against initial εNd and (b) initial γOs against initial εNd for Cretaceous oceanic plateaus. Data sources: Atlantic and Indian MORB—Salters (1996), Pacific—Nowell *et al.* (1998), Kerguelen plateau—Salters and Hart (1991), CCOP and Gorgona—Walker *et al.* (1999), Thompson *et al.* (2004), OJP—Babbs (1997).

the parental magmas of the CCOP has been calculated to be of the order of 20% (Kerr *et al.*, 1997a).

3.16.4.4 Ontong Java Plateau (~122 and ~90 Ma)

The Ontong Java plateau (OJP) in the western Pacific (Figure 1) has been tectonically uplifted and exposed along its south eastern margin, at the Solomon Islands arc, mostly on the Islands of Maliata and Santa Isabel. In contrast to the CCOP, which has numerous exposed sections, these are currently the only known subaerial exposures of the OJP. The rest of our knowledge of the OJP comes from a series of drill holes: DSDP Site 289 and ODP Sites 803 and 807 (Mahoney *et al.*, 1993a). Additional data are also now becoming available from ODP Leg 192 which recently penetrated the OJP at four sites (Mahoney *et al.*, 2001).

On Maliata the stratigraphic thickness of the accreted plateau reaches 3–4 km, and the succession is dominated by pillowed and massive basaltic flows (Petterson *et al.*, 1997; Babbs, 1997). Like the CCOP, dykes are volumetrically minor. The DSDP/ODP drill holes have penetrated into the plateau to a depth of 216 m (Site 1185B; Mahoney *et al.*, 2001). The sampled sections consist predominantly of pillowed and massive basalts with occasional thin interlava sediments (Neal *et al.*, 1997; Mahoney *et al.*, 2001)

In general, the OJP lavas are more homogeneous than those of the CCOP (Figures 5, 6 and 8). All the lavas from the province analyzed

thus far are basaltic in composition, with most of the samples possessing 6–8 wt.% MgO (Figures 5 and 6). Although the lavas of the OJP possess a restricted compositional range, they nonetheless fall into two compositionally distinct groups. These groups were first noted in the lavas from ODP Site 807, where Mahoney *et al.* (1993b) divided the lavas into different units (A and C-G). Unit A (A-Type) is chemically distinct from Units C-G (C-G-Type) and possesses higher levels of both incompatible elements (e.g., TiO_2; Sr, Zr Nb and the LREE; Figures 5–7) and ratios of highly incompatible to moderately incompatible trace elements (e.g., La/Y). The A-Type basalts also have lower initial εNd values and higher initial $^{87}Sr/^{86}Sr$ ratios than the C-G-Type (Figure 8(a)). However, the total range of εNd (+6.5 – +4.9) and $^{87}Sr/^{86}Sr$ (0.7034–0.7041) is relatively small in comparison with those in the CCOP (Figure 8(a)). The same is true for incompatible trace element ratios, with the OJP basalts only varying between 0.12 and 0.22 for La/Y and between 15.5–19.7 for Zr/Nb (Figure 6). However, recent analyses from ODP Leg 192 (Sites 1185 and 1187; on the eastern edge of the plateau) have revealed the occurrence of more-MgO-rich lavas (up to 11 wt.%) with higher Ni and Cr contents (Mahoney *et al.*, 2001; G. Fitton unpublished data; Figures 5 and 6). In addition to their higher MgO, preliminary geochemical data reveals that these basalts possess lower levels of incompatible elements (e.g., TiO_2: 0.72–0.77 and Zr: 36–43), than the A and C-G Types (Figures 5 and 6).

Neal *et al.* (1997) have concluded on the basis of geochemical modeling that the major and trace element compositions of the A- and C-G-type lavas of the OJP are consistent with 20–30% partial melting of a peridotite source. The more enriched nature of the A-Type lavas implies derivation form a slightly more enriched source region, possibly in conjunction with smaller degrees of melting. Mahoney *et al.* (2001) have proposed that the more MgO-rich, incompatible element-poor lavas discovered during Leg 192 represent more extensive melting of the plume source region. However, an alternative explanation is that these lavas were derived from a more depleted mantle source region, and radiogenic isotope data are required in order to resolve this issue. None of the compositions sampled thus far are magnesian enough to represent possible parental melts, and so are believed to have undergone 30–45% fractional crystallization, involving olivine, plagioclase and clinopyroxene (Neal *et al.*, 1997).

Although the deeper crustal and lithospheric levels of the OJP are not exposed, seismic velocity data has been used to model the crustal structure (Farnetani *et al.*, 1996; Gladczenko *et al.*, 1997). These authors have proposed that the magma chambers that fed the plateau are represented in the midcrust by olivine gabbros. These models also suggest that high compressional P-wave velocities of $>7.1\ km\ s^{-1}$ deep within the OJP are due to the presence of olivine and pyroxene cumulates produced by the fractionation of primary picritic melts. Alternatively, the high P-wave velocities could be due to the presence of garnet granulite deep in the plateau, which Gladczenko *et al.* (1997) suggested may have formed by deformation and hydrothermal alteration of lower crustal cumulates.

3.16.5 THE INFLUENCE OF CONTINENTAL CRUST ON OCEANIC PLATEAUS

Initially it may seem odd that the composition of oceanic plateaus should be influenced by continental crust, and certainly for the CCOP and the OJP, which apparently formed well away from continental margins, there is no evidence of the involvement of continental crust in their petrogenesis. However, LIPs can also form at the continent–ocean boundary as well as erupting onto either oceanic or continental lithosphere, and the formation of a LIP in such a tectonic setting is often related to continental break-up. The role played by mantle plumes in continental break-up (causal or consequential) remains controversial (White and McKenzie, 1989; Hill, 1991; Coffin and Eldholm, 1992; Saunders *et al.*, 1992; Barton and White, 1995). However, whether mantle plumes are the reason for or a result of continental break-up, the associated erupted lavas and intruded sills form thick magmatic sequences on the margins of the rifted continents: the so-called seaward-dipping reflector sequences (SDRS). These LIPs may also erupt on the adjacent continents to form continental flood basalt provinces. Furthermore, continuing plume-related magmatism combined with further separation of the continents ultimately results in the formation of oceanic plateaus. Two examples of provinces such as these are explored below: the North Atlantic Igneous Province (NAIP) and the Kerguelen plateau.

3.16.5.1 The North Atlantic Igneous Province (~60 Ma to Present Day)

The opening of the North Atlantic ~60 Ma is closely associated with magmatism from the "head" phase of the Icelandic plume. (For a comprehensive review of the NAIP see Saunders *et al.*, 1997). Much of the initial volcanism (Phase 1: 62–58 Ma; Saunders *et al.*, 1997) was confined to the continental margins, i.e., the on-land sequences in western Britain, the Faroe

Islands and east and west Greenland, as well as the seaward-dipping reflector sequences of the southeast Greenland margin and the Hatton Bank (Figure 10). Most of these lavas are contaminated with Archean-age continental crust and thus possess low εNd and high Ba/Nb (Figure 11), along with low $^{206}Pb/^{204}Pb$. As the North Atlantic continued to open, a second intense burst of magmatism occurred (beginning at 56 Ma; Phase 2, Saunders *et al.*, 1997). The lavas from this magmatism are preserved in the upper portions of the SDRS, off the coast of southeast Greenland and Western Europe and have been drilled by ODP Legs 104, 152 and 163 (Viereck *et al.*, 1988; Fitton *et al.*, 2000). In contrast to the Phase 1 lavas, these lavas show few signs of contamination by continental crust (low Ba/Nb; $\varepsilon Nd > 6$; (Figure 11) $^{206}Pb/^{204}Pb > 17$), indicating that by this time the NAIP was an entirely oceanic LIP. The Icelandic plume has been producing melt over most of the past 60 Myr, as evidenced by 55–15 Ma volcanism along the Greenland–Iceland ridge and the Faroes–Iceland ridge, and the 15 Ma–present volcanism on Iceland.

3.16.5.2 The Kerguelen Igneous Province (~133 Ma to Present Day)

The initial volcanism of the Kerguelen plume is closely associated with the break-up of Gondwana in the early–mid-Cretaceous, i.e., the separation of India, Australia and Antarctica (Morgan, 1981; Royer and Coffin, 1992). Like the NAIP, much initial volcanism is found on the margins of the rifted continents (Figure 12): the Rajmahal basalts in northeastern India (Kent *et al.*, 1997) and the Bunbury basalts in western Australia (Frey *et al.*, 1996). Not surprisingly, these basalts are extensively contaminated by continental lithosphere and yield an initial $^{87}Sr/^{86}Sr$ ratio of >0.7042 and $\varepsilon Nd < 4.0$ (Figure 13).

The geographical components of the plateau (Figure 12) and the geochronology are briefly outlined below; however, a more detailed review can be found in Frey *et al.* (2000); Coffin *et al.* (2002). The first massive pulse of Kerguelen plume magmatism created the Southern Kerguelen plateau (118–110 Ma; Figure 12). Later melting of the plume was responsible for

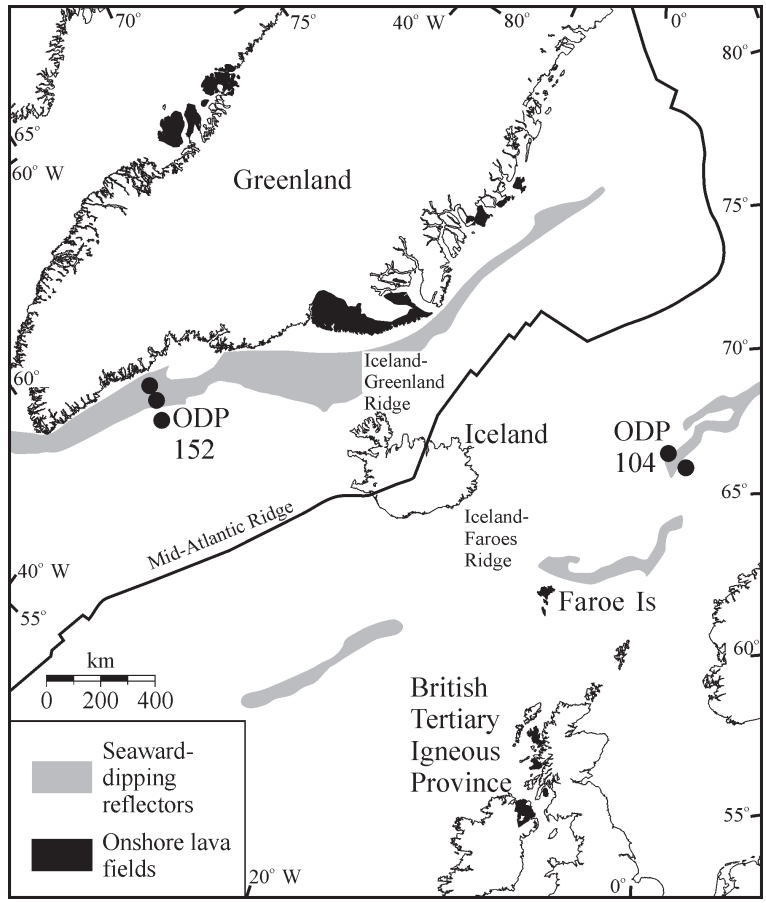

Figure 10 Map showing the locations of the principal on-land exposures of the North Atlantic Igneous Province and the seaward-dipping reflector sequences.

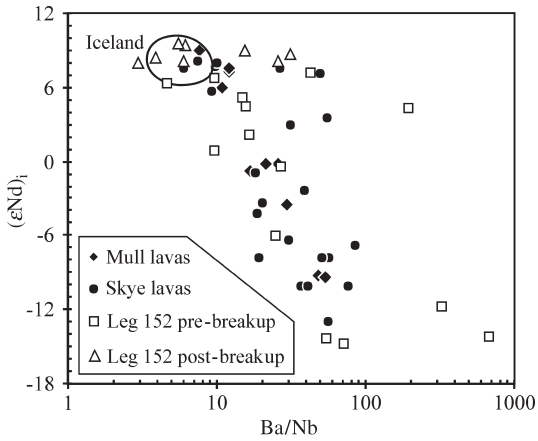

Figure 11 Plot of Ba/Nb vs. initial εNd lavas from the NAIP. Shown on the diagram are lavas from Skye (Thompson *et al.*, 1982; Dickin *et al.*, 1987), Mull (Kerr *et al.*, 1995), Iceland (Hémond *et al.*, 1993) and both pre- and post- continental break-up lavas from ODP Leg 152 (Fitton *et al.*, 1998a).

the formation of the Elan Bank (108–107 Ma), the Central Kerguelen Plateau (101–100 Ma), Broken Ridge (95–94 Ma), the Ninetyeast Ridge (82–37 Ma), and the Northern Kerguelen plateau (35–34 Ma) (Figure 12). Volcanism continues to the present-day and has produced the Kerguelen Archipelago and Heard and MacDonald Islands.

The lavas from the Southern Kerguelen plateau and Broken Ridge have initial $^{87}Sr/^{86}Sr$ ratios and εNd values (Figure 11) which range from 0.7037 to 0.7102 and +4.0 to −9.4, respectively (Salters *et al.*, 1992; Mahoney *et al.*, 1995). Some of this variation can be interpreted as mixing between Southeast Indian Ridge MORB and the Kerguelen plume (Weis and Frey, 1996). However, elevated La/Nb ratios (Figures 13 and 14(a)) and the extreme isotopic compositions of basalts drilled at ODP Site 738 and dredge samples from the eastern Broken Ridge ($^{87}Sr/^{86}Sr$ 0.710; εNd −9.0; Figures 8 and 13) cannot be explained by such mixing processes. It has been proposed that these signatures are due to contamination by continental lithosphere (Storey *et al.*, 1989; Mahoney *et al.*, 1995; Hassler and Shimizu, 1998). Operto and Charvis, 1996 have imaged a seismically reflective transition zone beneath the crust/mantle interface of the Southern Kerguelen plateau, interpreted as fragments of continental crust. This crust appears to have isotopic similarities to Archean crust found on the margins of Gondwana, which raises the possibility that fragments of such crust have become incorporated into the Indian Ocean basin during continental break-up. Recently, during drilling at Site 1137 on the Elan Bank (part of the Kerguelen plateau; Figure 12) clasts of garnet-biotite gneiss have been discovered in a fluvial conglomerate

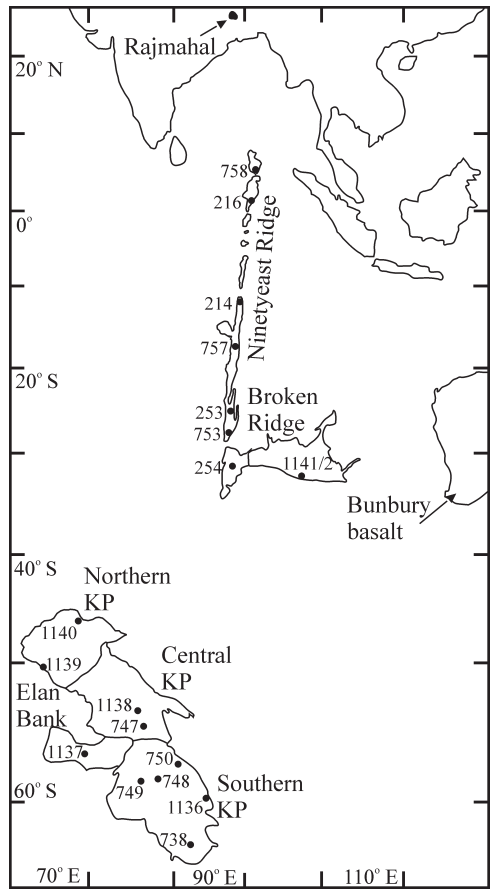

Figure 12 Map showing the main components of the Kerguelen plateau (KP) discussed in the text (after Frey *et al.*, 1996).

intercalated with basalt flows (Frey *et al.*, 2000). This discovery has confirmed the presence of pre-Cambrian crustal rocks within the Kerguelen plateau (Nicolaysen *et al.*, 2001), thus supporting the lithospheric contamination model for the high La/Nb, low εNd basalts of the Kerguelen plateau.

3.16.6 IDENTIFICATION OF OCEANIC PLATEAUS IN THE GEOLOGICAL RECORD

The rationale for this section is summed up by this question: If the CCOP or OJP were accreted on to a continental margin and preserved in the geologic record for 1 billion years, what features could we use to identify them as oceanic plateaus? This section will review diagnostic geochemical and geological characteristics of oceanic plateaus, and then will show, illustrated by examples, how these criteria can be used to identify plateau sequences in the geological record. Table 3 provides a summary of the diagnostic features of Cretaceous oceanic plateaus and mafic sequences

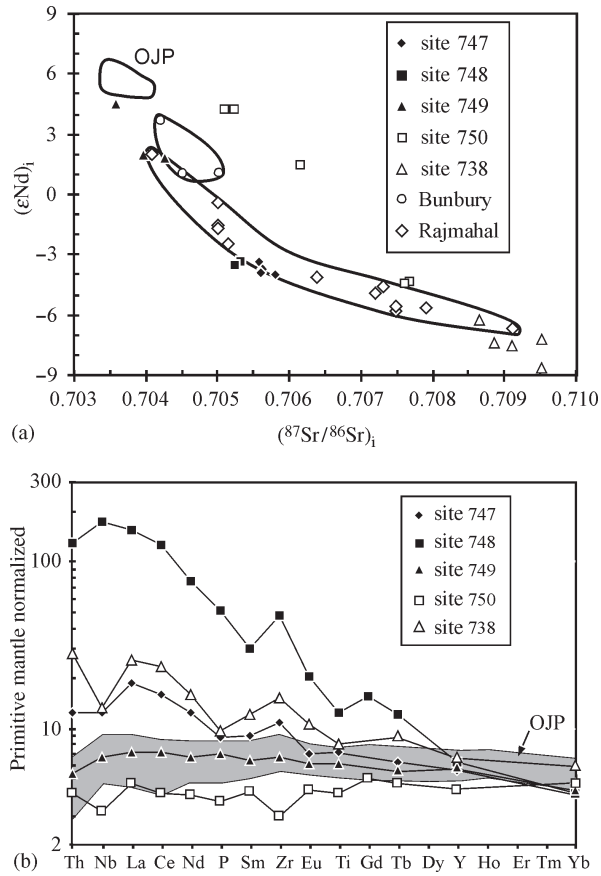

Figure 13 Plots to show the geochemical variation of lavas from the early Cretaceous lavas derived from the Kerguelen plume. (a) Initial $^{87}Sr/^{86}Sr$ vs. initial εNd and (b) primitive mantle normalized multi-element plots showing averaged data for ODP drill sites. A compositional field for the OJP (Mahoney *et al.*, 1993a,b) is shown on both diagrams. Data sources: Rajmahal—Kent *et al.* (1997); Bunbury—Frey *et al.* (1996); ODP sites—Salters *et al.* (1992); Mahoney *et al.* (1995).

within the continental crust, which have been interpreted as oceanic plateaus. Details of accreted oceanic plateaus thus far identified in the geological record are summarized in Table 4.

3.16.6.1 Diagnostic Features of Oceanic Plateaus

Both chemical and geological features can be useful in the identification of oceanic plateaus. Condie (1999) and Kerr *et al.* (2000) have discussed the diagnostic features of oceanic plateaus in detail, and only a brief account will be given here. Table 3 summarizes the characteristics which are useful in distinguishing igneous rocks formed in an oceanic plateau from those which originated in other tectonic settings.

Igneous rocks produced in an island arc, or a continental subduction zone setting, are relatively easily distinguished from oceanic plateau sequences (Table 3), because arcs generally possess more evolved lavas, with ubiquitous high $(La/Nb)_{pmn}$ ratios (Figure 14(b)), and only very rarely contain high-MgO lavas. Additionally, oceanic plateaus do not possess the abundant volcanic ash layers present in volcanic arc sequences. However, as Figure 14 shows, a low $(La/Nb)_{pmn}$ ratio is not an entirely robust signature of an oceanic plateau sequence, since samples of the Kerguelen oceanic plateau often possess high $(La/Nb)_n$ values, due to magma interaction with fragments of continental lithosphere beneath the plateau. This example highlights the importance of not relying solely on chemical discriminants of tectonic environment, without also considering the geological evidence. In the case of Kerguelen, the lack of volcaniclastic horizons helps confirm its oceanic plateau affinity. As discussed by Kerr *et al.* (2000), many of the geological discriminants between oceanic plateaus and midocean ridges may be ambiguous (Table 3). Geochemical characteristics must, therefore, be used to distinguish lavas from these two tectonic settings. Most Cretaceous oceanic plateau lavas possess relatively flat normalized REE patterns (Figure 7), whereas most midocean ridge basalts possess light REE-depleted patterns reflecting a more depleted

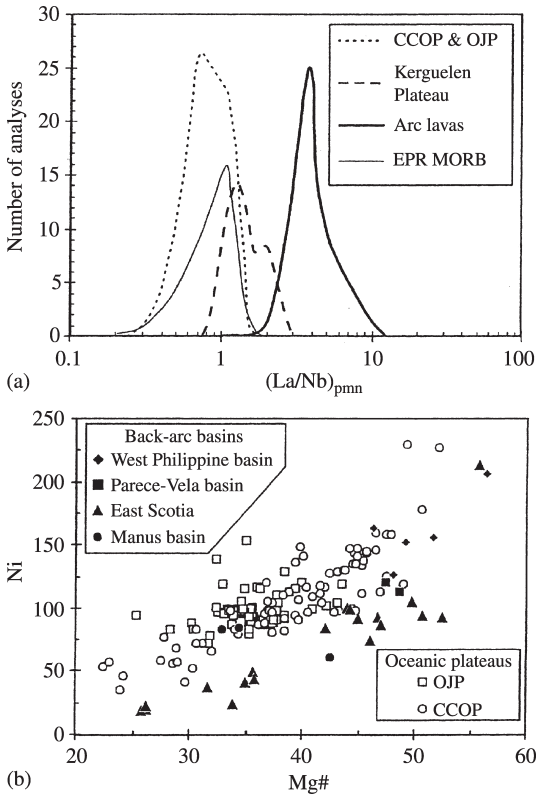

Figure 14 (a) Frequency diagram showing the range in $(La/Nb)_{pmn}$ for lavas from the CCOP–OJP, the Kerguelen plateau, EPR MORB, and arc lavas. (Arc data from Thirlwall *et al.*, 1996.) Other data sources as in Figures 5, 8 and 12). (b) Plot of Ni vs. Mg–number for the CCOP–OJP and lavas from back arc basins. Data from Wood *et al.* (1980), Woodhead *et al.* (1998), Leat *et al.* (2000). Both diagrams modified from Kerr *et al.* (2000).

mantle source region. Furthermore, high-MgO lavas can be found in oceanic plateaus, but are largely absent from oceanic crust generated at midocean ridges.

Incompatible trace elements are only of limited use in distinguishing between volcanic successions formed in back-arc basins and those formed in oceanic plateaus (Table 3). However, the lower mantle temperature below a back-arc basin ($T_p \sim 1{,}280\,^{\circ}C$) compared to a mantle plume ($T_p > 1{,}400\,^{\circ}C$) results in the eruption of few high-MgO lavas. An additional consequence of this lower mantle temperature is that back-arc basin lavas generally possess lower Ni and Cr contents for a given Mg number than oceanic plateau lavas (Figure 14(b)). Furthermore, because of their proximity to active subduction sites, back-arc basin sequences are also more likely to contain abundant volcaniclastic horizons than oceanic plateaus.

Continental flood basalts are not easy to preserve for long periods of time in the geological record simply because they are easily eroded away, unless they are buried by sediments. Quite often the only remaining indications of a continental flood basalt province are the dykes and vents through which the lavas erupted. The 200 Ma Central Atlantic Magmatic Province, which formed during the break-up of South America, Africa, and North America has been identified largely on the basis of its remnant dyke swarms (e.g., Marzoli *et al.*, 1999).

3.16.6.2 Mafic Triassic Accreted Terranes in the North American Cordillera

Significant proportions of the North American Cordillera consist of mafic sequences of accreted oceanic terranes (Figure 15). Some of these have been identified as oceanic plateau material ranging in age from Permian to Eocene (see review in Condie, 2001). At least three of these oceanic plateau terranes are predominantly Triassic in age (Wrangellia, Cache Creek and Angayucham; Pallister *et al.*, 1989; Lassiter *et al.*, 1995; Tardy *et al.*, 2001) and obviously represent a major phase of oceanic plateau volcanism at this time. These plateau sequences are characterized by pillow basalts and intrusive sheets, with occasional intercalated tephra and hyaloclastite layers, indicating formation in shallow water, or by subaerial eruption. In the Wrangellia terrane there is considerable evidence for rapid uplift of the sea floor (presumably by the plume head) immediately prior to eruption (Richards *et al.*, 1991).

The basalts of the Cache Creek and Angayucham terranes display a restricted range in MgO with most of the basalts ranging from 5.0 wt.% to 8.5 wt.%. These basalts possess low $(La/Nb)_{pmn}$ ratios (<1.2), essentially flat REE patterns (Pallister *et al.*, 1989; Tardy *et al.*, 2001) and εNd values that range mostly from +9.9 to +4.5 (Figure 16). As Figure 16 shows, all these features are similar to the OJP. However, some of the basalts from the Wrangellia Terrane, despite showing a similar range in MgO content, have $(La/Nb)_{pmn}$ ratios >1 and steeper REE patterns (Figure 16) than those from Cache Creek and Angayucham. Lassiter *et al.* (1995) suggested that this is due to the magmas erupting through, and being contaminated by preexisting island-arc lithosphere. However, it is also possible that, as in the case of the Kerguelen plateau, large fragments of ancient continental lithosphere were incorporated in the proto-Pacific Ocean, and the lavas of the Wrangellia oceanic plateau were contaminated by this lithosphere. The contamination of the most evolved Wrangellia basalts with either arc crust or ancient continental lithosphere is also supported by a broadly negative correlation between εNd and $(La/Nb)_{pmn}$ (Figure 16).

Table 3 Diagnostic geochemical and geological characteristics of volcanic sequences from different tectonic settings.

Tectonic setting	*High-MgO lavas (>14%)*	*Low-MgO lavas (<3%)*	$(La/Nb)_{pmn}$[a]	*Chondrite normalized REE pattern*	*Pillow lavas*	*Tephra layers*	*Subaerial eruption*	*Intercalated pelagic sediments*
Oceanic plateau	frequent	rare	≤1	Predominantly flat	yes	rare	occasional	yes
Midocean ridge	rare	rare	≤1	LREE-depleted	yes	rare	rare	no
Marginal basin	rare	rare	≤1	Predominantly flat	yes	yes	no	no
Oceanic island basalt	rare	rare	≤1	Predominantly LREE-enriched	yes	rare	frequent	rare
Volcanic rifted margin	frequent	rare	Varies from ≤1 to ≫1	Flat to LREE-enriched	not all lavas are pillowed	occasional	frequent	no
Arc (continental & oceanic)	rare	frequent	≫1	LREE-enriched	not all lavas are pillowed	yes	frequent	Rare
Continental flood basalt	frequent	frequent	mostly ≫ 1 < 10% of flows ≤1	Flat to LREE-enriched	no	occasional	yes	no

[a] pmn—primitive mantle normalized (after Kerr *et al.* 2000).

3.16.6.3 Carboniferous to Cretaceous Accreted Oceanic Plateaus in Japan

The Japanese islands are essentially composed of a series of terranes that have been accreted to the continental margin of the Eurasian plate during the past 400 Myr. These terranes consist of trench-filling terrigenous sediments with variable quantities of accreted oceanic crust that are intruded and partly overlain by the products of subsequent subduction-related volcanism. Within Japan the ages of the accreted complexes become younger from north to south and from west to east (Kimura *et al.*, 1994). However, relatively little is known about the trace element chemistry of these oceanic accreted terranes.

The Chugoku and Chichibu belts in southwest Japan contain up to 30% basaltic material (greenstones) in thrust contact with limestones, cherts and mudstones (Tatsumi *et al.*, 2000). This lithological association, combined with preliminary major element data and a small range of trace element data, suggests that these basaltic assemblages are remnants of a plume-derived oceanic plateau. Tatsumi *et al.* (2000) proposed that this oceanic plateau formed in the Panthalassan Ocean (proto-Pacific) in the Carboniferous (350–300 Ma).

The Permian Yakuno ophiolite complex in southern Honshu Island is a sequence of submarine basalts, gabbros and ultramafic rocks (Isozaki, 1997). The presence of pelagic sediments, the lack of a sheeted dyke complex and the fact that the sequence is of considerable thickness, all suggest that it is part of an oceanic plateau (Isozaki, 1997). In contrast to the other accretionary belts in Japan, the Sorachi-Anivia terrane in Hokkaido and Sakhalin is dominated by oceanic crust and lithosphere (Kimura *et al.*, 1994; Tatsumi *et al.*, 1998). It comprises pillow lavas and dolerite sills with intercalated pelagic sediments containing Tithonian (150–145 Ma) radiolaria, along with a lower unit in which ultramafic rocks, including serpentinite, harzburgite and dunite, are more common (Kimura *et al.*, 1994). Major element data have shown that some picrites (>12 wt.% MgO) are found within the succession. This, combined with high CaO/Al_2O_3 ratios (indicative of a high degree of mantle melting), led Kimura *et al.* (1994) and Tatsumi *et al.* (1998) to propose an oceanic plateau origin for the Sorachi-Anivia terrane. This Jurassic–early Cretaceous plateau (named the Sorachi plateau; Kimura *et al.*, 1994) is of the same age as the Shatsky Rise (Figure 1, Table 1). In combination with paleomagnetic data, this suggests that the Sorachi plateau and the Shatsky Rise were originally a single plateau which formed near the Kula–Pacific–Farallon triple junction ~150 Ma (Kimura *et al.*, 1994).

Table 4 Proposed accreted oceanic plateaus found within continents.

Name	*Location*	*Age (Ga)*	*References*
Coonterunah and Warrawoona Groups	Pilbara Craton, Australia	~3.5	Green *et al.* (2000)
Southern Barberton Belt	Kaapvaal Craton, S Africa	3.5–3.2	De Wit *et al.* (1987)
Pietersberg Belt	Kaapvaal Craton, S Africa	~3.4	De Wit *et al.* (1987)
Opapimiskan-Markop Unit, North Caribou Belt[a]	Superior Province	~3.0	Hollings and Wyman (1999)
Olondo Belt	Aldan Shield, Siberia	3.0	Puchtel and Zhuravlev (1993); Bruguier (1996)
South Rim Unit, North Caribou Belt	Superior Province	~3.0	Hollings and Wyman (1999)
Sumozero-Kenozero Belt	Baltic Shield	3.0–2.8	Puchtel *et al.* (1999)
Steep Rock & Lumby Lake Belts[a]	Superior Province	3.0–2.9	Tomlinson *et al.* (1999)
Balmer Assemblage, Red Lake Greenstone Belt[a]	Superior Province	2.99–2.96	Tomlinson *et al.* (1998)
Kostomuksha Belt	Baltic Shield	2.8	Puchtel *et al.* (1998b)
Vizien Belt	Superior Province	2.79	Skulski and Percival (1996)
Malartic-Val d'Or Area	Superior Province	2.7	Kimura *et al.* (1993); Desrochers *et al.* (1993)
Tisdale Group, Abitibi Belt	Superior Province	~2.7	Fan and Kerrich (1997)
Schreiber-Hemlo-White River Dayohessarah	Superior Province	2.8–2.7	Polat *et al.* (1998)
Vetreny Belt[a]	Baltic Shield	2.44	Puchtel *et al.* (1997)
Birimian Province	West Africa	2.2	Abouchami *et al.* (1990); Boher *et al.* (1992)
Povungnituk & Chukotat Groups[a]	Cape Smith Fold Belt Northern Québec	2.04	Francis *et al.* (1983); Dunphy *et al.* (1995)
Onega Plateau[a]	Baltic Shield	1.98	Puchtel *et al.* (1998a)
Jormua Ophiolite[a]	NE Finland	1.95	Peltonen *et al.* (1996)
Flin Flon Belt	Central Canada	1.92–1.90	Lucas *et al.* (1996); Stern *et al.* (1995)
Arabian-Nubian Shield	NE Africa-Middle East	0.90-0.87	Stein and Goldstein (1996)
Chichibu & Chugoku Belts	SW Japan	Carboniferous	Tatsumi *et al.* (2000)
Yakuno Ophiolite	SW Japan	0.285	Isozaki (1997)
Mino Terrane	Central Japan	L Permian	Jones *et al.* (1993)
Cache Creek Terrane	Canadian Cordillera	Triassic	Tardy *et al.* (2001)
Angayucham Terrane	Alaska	Triassic	Pallister *et al.* (1989)
Wrangellia Terrane	Western North America	0.227	Lassiter *et al.* (1995).
Sorachi Plateau	Northern Japan	0.152–0.145	Kimura *et al.* (1994); Tatsumi *et al.* (1998)

[a] These sequences display evidence of contamination by continental crust and are interpreted as having formed during continental break-up or, close to a continental margin (see text).

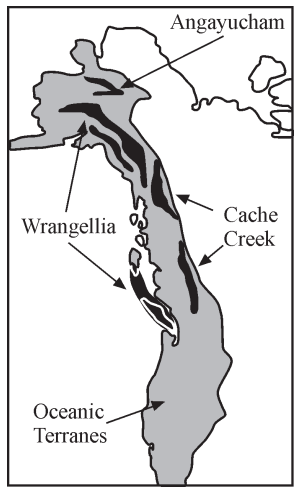

Figure 15 Map showing North American accreted oceanic terranes including the oceanic plateau sequences discussed in the text (after Tardy *et al.*, 2001; Condie, 2001).

The Sorachi part of the plateau was carried northwestwards on the Kula plate and collided with Japan ~110 Ma. Limited trace element data for the Sorachi plateau lavas support a common plume source for these two plateaus. The data cover the same compositional range as that of dredged samples from the Shatsky Rise (Figure 17). Furthermore, the data reveal that the plume source region of the Sorachi plateau was markedly heterogeneous and contained both enriched and depleted components (Kimura *et al.*, 1994; Tatsumi *et al.*, 1998) (Figure 17).

3.16.7 PRECAMBRIAN OCEANIC PLATEAUS

The identification of accreted pre-Cambrian oceanic plateaus, particularly in greenstone belts, has important implications for the generation of continental crust (Abbott, 1996; Albarede, 1998; Condie, 1999). Kerr *et al.* (2000) have presented

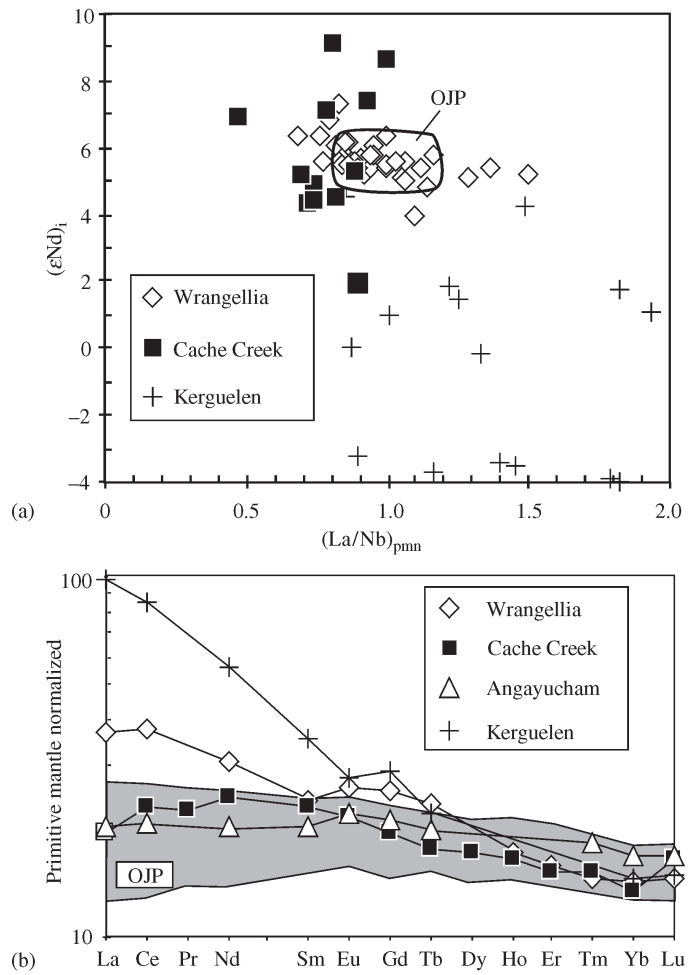

Figure 16 Plots of (a) $(La/Nb)_{pmn}$ against initial εNd for Cache Creek, Wrangellia, OJP and the Kerguelen plateau and (b) chondrite normalized (Sun and McDonough, 1989) REE plot showing averages for Wrangellia, Angayucham, Cache Creek, and the Kerguelen plateau, with the range for the OJP. Data sources are as in Figures 5 and 12; North American data from Pallister *et al.* (1989); Lassiter *et al.* (1995); and Tardy *et al.* (2001).

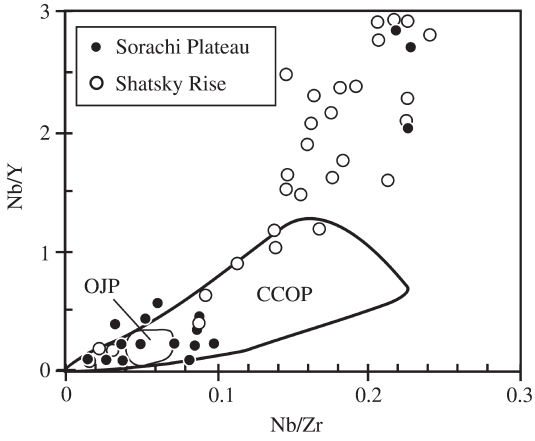

Figure 17 Plot of Nb/Y against Nb/Zr showing data from dredge samples from the Shatsky Rise and the accreted Sorachi plateau (data from Tatsumi *et al.*, 1998). Also shown are fields for the CCOP and OJP. Data sources are as in Figure 5.

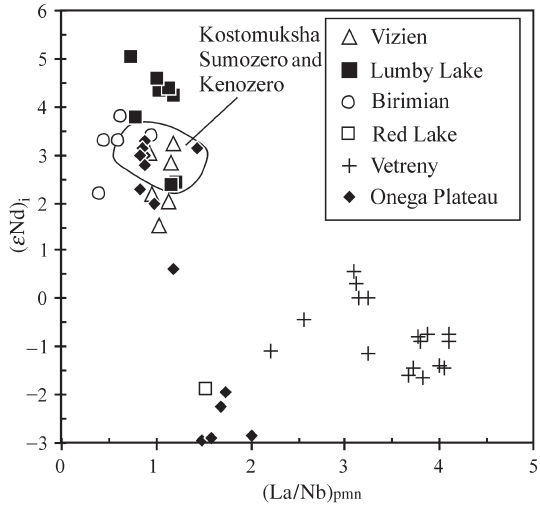

Figure 18 Plot of $(La/Nb)_{pmn}$ vs. initial εNd for data from Archean and Proterozoic accreted oceanic plateaus and provinces proposed to have formed during continental rifting. Data sources: Abouchami *et al.* (1990); Skulski and Percival (1996); Puchtel *et al.* (1998a); Tomlinson *et al.* (1998); Hollings and Wyman (1999).

a summary of accreted pre-Cambrian oceanic plateaus and the reader is referred to their paper for more detailed information.

Some of the oldest preserved oceanic plateau sequences are those found in ~3.5 Ga Barberton and Pietersberg belts of the Kaapvaal Shield of southern Africa (De Wit *et al.*, 1987; Smith and Erlank, 1982). These belts contain pillow basalts and komatiites, with chemical signatures (Lahaye *et al.*, 1995) suggesting a likely origin as part of an oceanic plateau. The Pilbara craton of Australia appears to possess some of the oldest oceanic plateau material so far identified (Green *et al.*, 2000) in the ~3.5 Ga Coonterunah and Warrawoona Groups.

Greenstone belts of the Canadian Superior province, ranging in age from 3.0 to 2.7 Ga also contain lava groups that have been interpreted to be remnants of accreted oceanic plateaus. These belts include the South Rim unit of the North Caribou belt (Hollings and Wyman, 1999), the Vizien belt (Skulski and Percival, 1996), the Malartic-Val d'Or (Desrochers *et al.*, 1993), the Tisdale Group of the Abitibi belt (Fan and Kerrich, 1997), and the Schreiber-Hemlo and the White River-Dayohessarah belts (Polat *et al.*, 1998). The evidence for an oceanic plateau origin is based on the occurrence of pillow basalts and komatiites without terrestrial sedimentary intercalations or sheeted dyke swarms, possessing low $(La/Nb)_{pmn}$ and the low positive εNd (Figure 18) that are characteristic of Cretaceous oceanic plateaus. Several of these sequences within the Superior province are in stratigraphic contact with basalts and komatiites that possess a signature of continental lithosphere contamination, i.e., negative εNd and $(La/Nb)_{pmn} > 1$ (Figure 18). These include the Balmer assemblage, Red Lake belt (Tomlinson *et al.*, 1998), Steep Rock-Lumby Lake belts (Tomlinson *et al.*, 1999), and Opapimiskan-Markop unit, North Caribou belt (Hollings and Wyman, 1999). These sequences have been interpreted as having formed in tectonic settings related to continental break-up, similar to the North Atlantic Tertiary igneous province and parts of the Cretaceous Kerguelen plateau.

Puchtel *et al.* (1998b, 1999) have proposed that the 3.0–2.8 Ga Kostomuksha and Sumozero-Kenozero greenstone belts of the Baltic Shield represent remnants of oceanic plateaus. This interpretation is based on the occurrence of crustally uncontaminated pillow basalts (Figure 18) and komatiites without terrestrial sedimentary intercalations. In contrast the 2.4 Ga Vetreny greenstone belt and the 1.98 Ga Onega plateau, also part of the Baltic Shield, display chemical evidence of crustal contamination (negative εNd; Figure 18). These sequences were interpreted by Puchtel *et al.* (1997, 1998a) as having formed during continental break-up.

Other Proterozoic oceanic plateau terranes have been identified in the Birimian province of western Africa (Figure 18) (Abouchami *et al.* 1990; Boher *et al.*, 1992), the Arabian-Nubian Shield (Stein and Goldstein, 1996), and the Flin Flon belt in Canada (Stern *et al.*, 1995).

3.16.8 ENVIRONMENTAL IMPACT OF OCEANIC PLATEAU FORMATION

Although the potential environmental impact of continental flood basalt provinces has been

documented by many authors (e.g., Hallam, 1987a; McLean, 1985; Renne and Basu, 1991; Courtillot *et al.*, 1996), the possible effects of oceanic plateau eruptions on the atmosphere, biosphere and hydrosphere have received comparatively little attention (see, for example, Courtillot, 1994). This omission is surprising since the inclusion of oceanic plateau events actually strengthens the correlation between LIP eruptions and mass extinction events (Kerr, 1997), by providing a feasible terrestrial causal mechanism for several second order extinction events (Sepkoski, 1986).

3.16.8.1 Cenomanian–Turonian Boundary (CTB) Extinction Event

Several of these second order extinction events occurred in the mid-Cretaceous. One of these, the CTB event (~93 Ma) has been linked by several authors to the formation of oceanic plateaus (Sinton and Duncan, 1997; Kerr, 1998). The CTB event is characterized by the world-wide deposition of organic-rich black shales (Jenkyns, 1980; Schlanger *et al.*, 1987). The formation of black shale implies a widespread reducing environment ("anoxia") in the oceans at this time (Figure 19). In addition to this, the CTB was a time of major sea level transgression (Hallam, 1989) and is marked by a positive carbon isotopic anomaly ($\delta^{13}C$ excursion) of up to +4–5‰ (Arthur *et al.*, 1987), indicating an increase in organic carbon burial rate (Figure 19). Sea water $^{87}Sr/^{86}Sr$ (Figure 19) reaches a maximum of 0.70753 in the late-Cenomanian, and drops steadily to a value of 0.70737 in the mid-Turonian, before starting to rise again. Average global surface temperatures (including oceanic temperatures) around the CTB were 6–14 °C higher than present (Kaiho, 1994), and this is most likely due to an increase in global atmospheric CO_2 content which may have been >10 times present-day levels (Figure 19) (Arthur *et al.*, 1987).

These phenomena were accompanied by an extinction event that resulted in the demise of 26% of all known genera (Sepkoski, 1986). Although the overall extinction rate is much lower than that at the Cretaceous–Tertiary boundary, deep water marine invertebrates fared much worse in the CTB event (Kaiho, 1994). This difference supports the view that anomalous oceanic volcanism around the CTB may have played a significant role in the environmental and biotic crisis at this time (Kerr, 1998).

Siderophile and compatible lithophile trace elements such as Sc, Ti, V, Cr, Mn, Co, Ni, Pt, Ir and Au are enriched in CTB black shales (Leary and Rampino, 1990; Orth *et al.*, 1993). Kerr (1998) has shown that trace element abundances and ratios found in CTB black shales are similar to plume-derived volcanic rocks and midocean ridge basalts. For example, in mafic volcanic rocks $Ni/Ir \times 10^4$ values range from 70 to 190, and in CTB sediments this ratio averages 180. In contrast, average sedimentary rocks possess $Ni/Ir \times 10^4$ ratios of ~100 (Orth *et al.*, 1993).

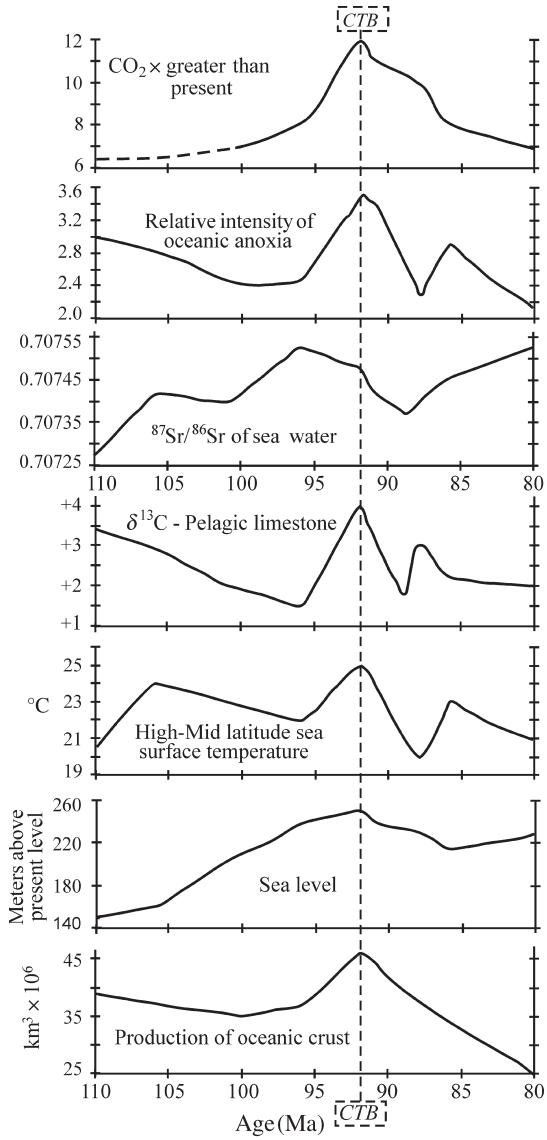

Figure 19 Graphs showing how various parameters discussed in the text vary from 110 Ma to 80 Ma. The dotted vertical line represents the Cenomanian–Turonian boundary (after Kerr, 1998).

3.16.8.2 Links between CTB Oceanic Plateau Volcanism and Environmental Perturbation

The most extensive plume-related volcanism around the CTB occurred in the oceans, with

the formation of the CCOP along with portions of the OJP and Kerguelen plateau. In addition to this oceanic volcanism, a continental flood basalt province related to the Marion hotspot also erupted at this time, as Madagascar rifted from India (Storey *et al.*, 1995). The estimated erupted volume of oceanic plateau lavas around this time is $\sim 1.0 \times 10^7$ km^3 and may be much higher (Kerr, 1998). The potential physical and chemical effects of oceanic plateau volcanism on the global environment are summarized in Figure 20 and discussed below.

An obvious physical effect of oceanic mantle plume volcanism is to raise sea level by lava extrusion onto the ocean floor through the buoyant plume head uplifting the oceanic lithosphere and displacing seawater (Courtney and White, 1986) and by the thermal expansion of seawater due to heating. The steady rise in global sea level throughout the Late Albian and Cenomanian (Figure 19) may reflect the arrival of the Caribbean, Ontong Java and Kerguelen plume heads below the oceanic lithosphere, prior to extensive volcanism (Vogt, 1989; Larson, 1991). This plume-related uplift of oceanic lithosphere may also have caused the disruption of important oceanic circulation systems such that cool, polar (oxygenated) waters were not circulated to lower latitudes, resulting in increased oceanic anoxia. Additionally, hydrothermal fluids from oceanic plateau volcanism could have contributed to warmer oceans, and thus to anoxia, since oxygen

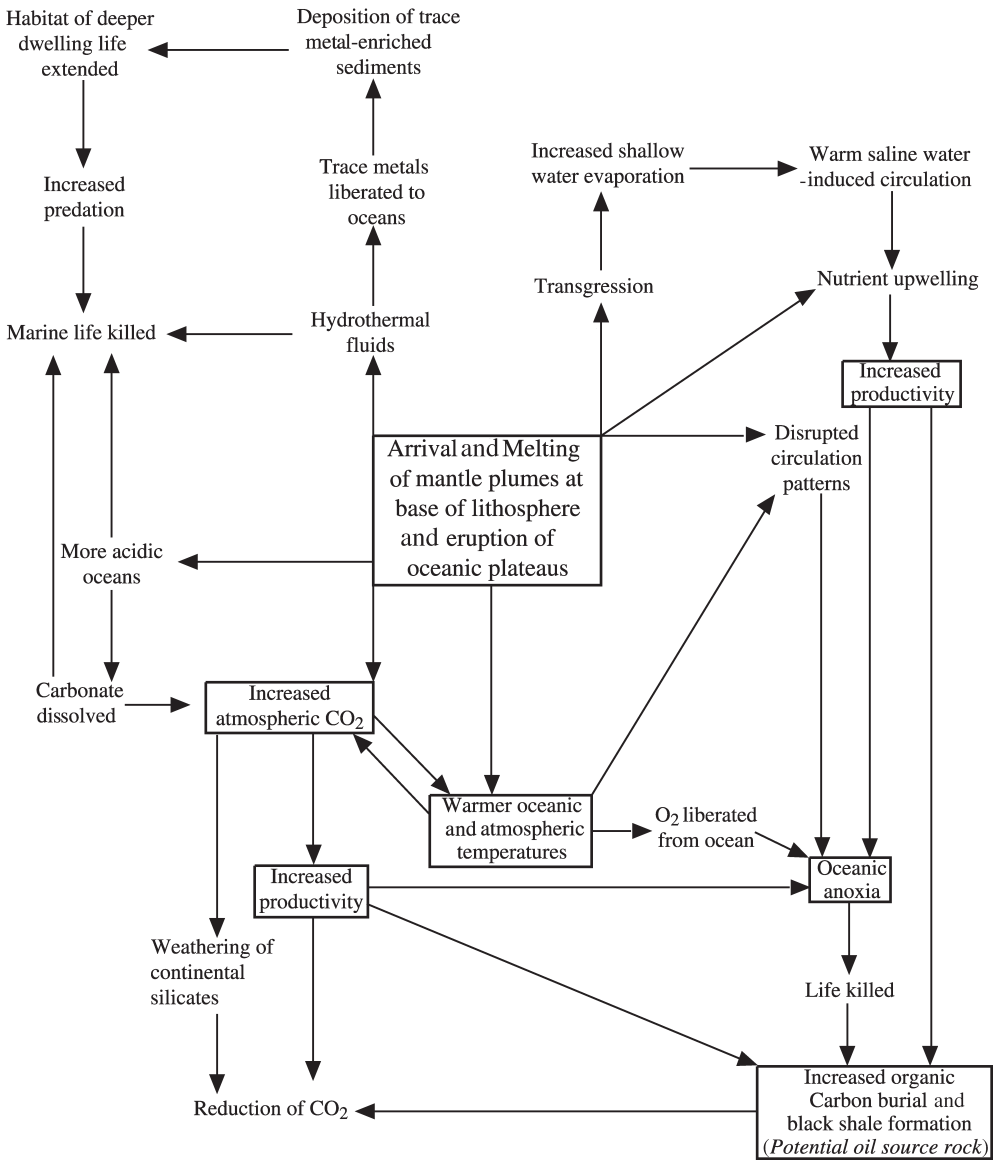

Figure 20 Flow diagram summarizing the possible physical and chemical environmental effects of the formation of large igneous provinces around the Cenomanian–Turonian boundary (after Kerr, 1998).

solubility is considerably reduced in warmer seawater (Sinton and Duncan, 1997).

Positive $\delta^{13}C$ anomalies at the CTB reflect increased rates of organic carbon burial as a result of high productivity and more effective preservation of organic material (Arthur *et al.*, 1987). Such increased productivity means the supply of deep ocean nutrients, such as phosphates, into surface waters must also increase and this process may have been induced by oceanic plateau volcanism (Vogt, 1989; Sinton and Duncan, 1997).

Elevated CO_2 levels at the CTB may also be due to increased volcanic activity. Kerr (1998) has calculated that approximately 10^{17} kg of CO_2 would have been released as a result of oceanic plateau volcanism around the CTB (Arthur *et al.*, 1987). Additionally, LIP volcanism also releases substantial amounts of SO_2, chlorine, fluorine and H_2S which, when released into seawater, would have made the CTB oceans much more acidic (Kerr, 1998). The lack of carbonate at the CTB may be the result of increased dissolution by more acidic seawater, which would also release more CO_2 to the atmosphere (Arthur *et al.*, 1987).

These additions of CO_2 to the atmosphere would have resulted in significant global warming. The solubility of CO_2 in seawater decreases as the temperatures rise; so the warmer the oceans get, the less CO_2 will dissolve in them. Thus, with this positive CO_2 feedback mechanism it is possible that a "runaway greenhouse" climate may have developed quite rapidly (Figure 20) (Kerr, 1998). Increased weathering of continental silicates can reduce CO_2 levels. However, the rate of CO_2 release at the CTB was much greater than its uptake by slow weathering processes. Increased atmospheric CO_2 and the upwelling of nutrients from the deep ocean could have resulted in increased productivity in ocean surface waters (Figure 20), leading to the widespread deposition of black shales and thus a reduction in CO_2 levels.

Increased concentration of toxic trace metals in the oceans, liberated by hydrothermal fluids from oceanic plateau lava piles, may well have been a contributory factor to the demise of some marine organisms around the CTB (Wilde *et al.*, 1990). The upwelling of deep ocean trace metals and nutrients may result in the enlargement of the trace metal-restricted habitat of deeper dwelling organisms (Wilde *et al.*, 1990), leading to increased predation by deeper dwelling creatures on those living in shallower water.

Throughout the past 250 Myr significant black shale deposits occur during several other periods and, like the CTB, these other black shales are associated with, sometimes severe, environmental disruption (Jenkyns, 1980; Hallam, 1987b; Arthur and Sageman, 1994). It is interesting, and probably highly significant, that these black shale events correlate with the formation of oceanic plateaus or plume-related volcanic rifted margins (Table 5). The Aptian–Albian (121–99 Ma) appears to have been a period of persistent environmental disturbance with three distinct oceanic anoxia events (with associated black shales) during this period (Bralower *et al.*, 1993). A causal link between black shale formation, environmental perturbation and oceanic volcanism is given further credence by the fact that a major period of oceanic plateau formation occurred during the Aptian–Albian (121–98 Ma) (see above).

Finally, Condie *et al.* (2001) have presented evidence that the correlation between black shale deposition, paleoclimatic disturbance and mantle superplume events can be extended back to the pre-Cambrian. Particularly good correlations between environmental disturbance and mantle plume activity occur at 1.9 Ga and 2.7 Ga

3.16.9 CONCLUDING STATEMENTS

Oceanic plateaus represent overthickened areas of oceanic crust (10–35 km), which appear to have formed as a result of decompression melting of a large mantle plume head, often (although not always) within 1–2 Ma. Geological and geochemical evidence suggests that oceanic plateaus have formed throughout a considerable period of Earth's history.

The thickness of the crustal sections of oceanic plateaus implies that they are not easily subducted. Thus, when these plateaus encounter a subduction zone, their top-most portions tend to become

Table 5 Correlations between black shale events and oceanic plateau volcanism over the last 250 Ma.

Age	*Black shales*	*Oceanic plateau or volcanic rifted margin*
Aptian–Albian (121–99 Ma)	Extensive world-wide deposits	Ontong Java & other Pacific plateaus, Kerguelen
Tithonian (150–144 Ma)	Extensive deposits in Europe and west Asia	Sorachi plateau & Shatsky Rise
Toarcian (190–180 Ma)	Extensive world-wide deposits	Karoo, Ferrar & Weddell Sea
Carnian (227–220 Ma)	Few deposits	Wrangellia

Data sources: Hallam (1987b); Jenkyns (1980); Riley and Knight (2001); Hergt and Brauns (2001).

accreted to a continent or an island arc. In this way fragments of oceanic plateaus have become incorporated into continental margins and preserved in the geological record.

Two recent examples of such accreted oceanic plateaus are the CCOP and the OJP. All of the lavas sampled from the OJP and most of the lavas from the CCOP are relatively homogeneous basalts with initial εNd values between +5 and +8 and broadly chondritic trace element ratios. In contrast, high-MgO lavas found in the CCOP reveal evidence of a more heterogeneous plume source region, containing both enriched ($\varepsilon Nd < +5$; $(La/Nd)_{cn} > 1$) and depleted ($\varepsilon Nd < +8$; $(La/Nd)_{cn} < 1$) components.

The formation of LIPs during continental break-up (e.g., the NAIP and the Kerguelen plateau) results in the formation of seaward-dipping reflector sequences and oceanic plateaus, both of which show chemical evidence of contamination by ancient continental lithosphere (initial $\varepsilon Nd < 0$; $(La/Nb)_{pmn} > 1$).

The correlation between oceanic plateau formation and marine environmental catastrophes (characterized by mass extinction, oceanic anoxia and black shale deposition) throughout the Mesozoic period suggests a causal link between oceanic plateau formation and environmental crises.

REFERENCES

Abbott D. H. (1996) Plumes and hotspots as sources of greenstone belts. *Lithos* **37**, 113–127.

Abouchami W., Boher M., Michard A., and Albarede F. (1990) A major 2.1 Ga event of mafic magmatism in West Africa—an early stage of crustal accretion. *J. Geophys. Res.* **95**, 17605–17629.

Aitken B. G. and Echeverría L. M. (1984) Petrology and geochemistry of komatiites and tholeiites from Gorgona Island, Colombia. *Contrib. Mineral. Petrol.* **86**, 94–105.

Albarede F. (1998) The growth of continental crust. *Tectonophysics* **296**, 1–14.

Arndt N. T., Kerr A. C., and Tarney J. (1997) Dynamic melting in plume heads: the formation of Gorgona komatiites and basalts. *Earth Planet. Sci. Lett.* **146**, 289–301.

Arthur M. A. and Sageman B. B. (1994) Marine black shales—depositional mechanisms and environments of ancient deposits. *Ann. Rev. Earth Planet. Sci.* **22**, 499–551.

Arthur M. A., Schlanger S. O., and Jenkyns H. C. (1987) The Cenomanian–Turonian Oceanic Anoxic Event: II. In *Paleoceanographic Controls on Organic-matter Production and Preservation,* Geological Society of London Special Publication 26 (eds. J. Brooks and A. J. Fleet), pp. 401–420.

Babbs T. L. (1997) Geochemical and petrological investigations of the deeper portions of the Ontong Java Plateau: Maliata, Solomon Islands. PhD Thesis, University of Leicester, UK, (unpublished).

Barton A. J. and White R. S. (1995) The Edoras Bank margin: continental break-up in the presence of a mantle plume. *J. Geol. Soc. London* **152**, 971–974.

Ben-Avraham Z., Nur A., Jones D., and Cox A. (1981) Continental accretion: from oceanic plateaus to allochthonous terranes. *Science* **213**, 47–54.

Bence A. E., Papike J. J., and Ayuso R. A. (1975) Petrology of submarine basalts from the Central Caribbean: DSDP Leg 15. *J. Geophys. Res.* **80**, 4775–4804.

Boher M., Abouchami W., Michard A., Albarede F., and Arndt N. T. (1992) Crustal Growth in West Africa at 2.1 Ga. *J. Geophys. Res.-Solid Earth* **97**, 345–369.

Bralower T. J., Sliter W. V., Arthur T. J., Lekie R. M., Allard D. J., and Schlanger S. O. (1993) Dysoxic/anoxic events in the Aptian–Albian (Early Cretaceous). In *The Mesozoic Pacific: Geology, Tectonics, and Volcanism,* American Geophysical Union Monograph 77 (eds. M. S. Pringle, W. W. Sager, W. V. Sliter, and S. Stein), pp. 5–37.

Bruguier O. (1996) U–Pb ages on single detrital zircon grains from the Tasmiyele group: implications for the evolution of the Olekma block (Aldan shield, Siberia). *Precamb. Res.* **78**, 197–210.

Burke K. (1988) Tectonic evolution of the Caribbean. *Ann. Rev. Earth Planet. Sci.* **16**, 201–230.

Caldeira K. and Rampino M. R. (1990) Deccan volcanism, greenhouse warming, and the Cretaceous/Tertiary boundary. In *Global Catastrophes in Earth History,* Geological Society of America Special Paper 247 (eds. V. L. Sharpton and P. D. Ward), pp. 117–123.

Campbell I. H. and Griffiths R. W. (1990) Implications of mantle plume structure for the evolution of flood basalts. *Earth Planet. Sci. Lett.* **99**, 79–93.

Campbell I. H., Griffiths R. W., and Hill R. I. (1989) Melting in an Archaean mantle plume: heads it's basalts, tails it's komatiites. *Nature* **339**, 697–699.

Cloos M. (1993) Lithospheric buoyancy and collisional orogenesis: subduction of oceanic plateaus, continental margins, island arcs, spreading ridges, and seamounts. *Geol. Soc. Am. Bull.* **105**, 715–737.

Coffin M. F. (1994) Large igneous provinces: crustal structure, dimensions, and external consequences. *Rev. Geophy.* **32**, 1–36.

Coffin M. F. and Eldholm O. (1992) Volcanism and continental break-up: a global compilation of large igneous provinces. In *Magmatism and the Causes of Continental Breakup,* Geological Society of London Special Publication 68 (eds. B. C. Storey, T. Alabaster, and R. J. Pankhurst), pp. 17–30.

Coffin M. F., Pringle M. S., Duncan R. A., Gladczenko T. P., Storey M., Muller R. D., and Gahagan L. A. (2002) Kerguelen hotspot magma output since 130 Ma. *J. Petrol.* **43**, 1121–1139.

Condie K. C. (1999) Mafic crustal xenoliths and the origin of the lower continental crust. *Lithos* **46**, 95–101.

Condie K. C. (2001) *Mantle Plumes and their Record in Earth History*. Cambridge University Press.

Condie K. C., Marais D. J. D., and Abbott D. (2001) Precambrian superplumes and supercontinents: a record in black shales, carbon isotopes, and paleoclimates? *Precamb. Res.* **106**, 239–260.

Courtillot V. (1994) Mass extinctions in the last 300 million years: one Impact and seven flood basalts? *Isr. J. Earth Sci.* **43**, 255–266.

Courtillot V., Jaeger J. J., Yang Z. Z., Feraud G., and Hofmann C. K. B. (1996) The influence of continental flood basalts on mass extinctions: where do we stand? In *The Cretaceous–Tertiary Event and Other Catastrophes in Earth History,* Geological Society of America Special Paper 307 (eds. G. Ryder, D. Fastovsky, and S. Gartner), pp. 513–525.

Courtney R. and White R. (1986) Anomalous heat flow and geoid across the Cape Verde Rise: evidence for dynamic support from a thermal plume in the mantle. *Geophys, J. Roy. Astr. Soc.* **87**, 815–867.

De Wit M. J., Hart R. A., and Hart R. J. (1987) The Jamestown ophiolite complex Barberton mountain belt: a section through 3.5 Ga oceanic crust. *J. Afr. Earth Sci.* **6**, 681–730.

Desrochers J. P., Hubert C., Ludden J. N., and Pilote P. (1993) Accretion of Archean Oceanic Plateau fragments in the Abitibi Greenstone Belt, Canada. *Geology* **21**, 451–454.

Dickin A. P., Jones N. W., Thirlwall M. F., and Thompson R. N. (1987) A Ce/Nd isotope study of crustal contamination processes affecting Palaeocene magmas in Skye, Northwest Scotland. *Contrib. Mineral. Petrol.* **96**, 455–464.

Donnelly T. W. (1973) Late Cretaceous basalts from the Caribbean, a possible flood basalt province of vast size. *EOS* **54**, 1004.

Dunphy J. M., Ludden J. N., and Francis D. (1995) Geochemistry of mafic magmas from the Ungava Orogen, Quebec, Canada and implications for mantle reservoir compositions at 2.0 Ga. *Chem. Geol.* **120**, 361–380.

Dupré B. and Echeverría L. M. (1984) Pb Isotopes of Gorgona Island (Colombia): isotopic variations correlated with magma type. *Earth Planet. Sci. Lett.* **67**, 186–190.

Echeverría L. M. (1980) Tertiary or Mesozoic komatiites from Gorgona Island, Colombia: field relations and geochemistry. *Contrib. Mineral. Petrol.* **73**, 253–266.

Edgar N. T., Ewing J. I., and Hennion J. (1971) Seismic refraction and reflection in the Caribbean Sea. *Am. Assoc. Petrol. Geol.* **55**, 833–870.

Eldholm O. and Coffin M. F. (2000) Large igneous provinces and plate tectonics. *AGU Monograph* **121**, 309–326.

Fan J. and Kerrich R. (1997) Geochemical characteristics of aluminum depleted and undepleted komatiites and HREE-enriched low-Ti tholeiites, western Abitibi greenstone belt: a heterogeneous mantle plume convergent margin environment. *Geochim. Cosmochim. Acta* **61**, 4723–4744.

Farnetani D. G. and Richards M. A. (1995) Thermal entrainment and melting in mantle plumes. *Earth Planet. Sci. Lett.* **136**, 251–267.

Farnetani C. G., Richards M. A., and Ghiorso M. S. (1996) Petrological models of magma evolution and deep crustal structure beneath hotspots and flood basalt provinces. *Earth Planet. Sci. Lett.* **143**, 81–94.

Fitton J. G., Saunders A. D., Norry M. J., Hardarson B. S., and Taylor R. N. (1997) Thermal and chemical structure of the Iceland plume. *Earth Planet. Sci. Lett.* **153**, 197–208.

Fitton J. G., Hardarson B. S., Ellam R., and Rogers G. (1998a) Sr-, Nd-, and Pb-isotopic composition of volcanic rocks from the Southeast Greenland margin at 63 degrees N: temporal variation in crustal contamination during continental breakup. *Proc. ODP Sci. Results* **152**, 351–357.

Fitton J. G., Saunders A. D., Larsen H. C., Hardarson B. S., and Norry M. J. (1998b) Volcanic rocks from the East Greenland margin at 63°N: composition, petrogenesis and mantle sources. In *Proceedings of the Ocean Drilling Program, Scientific Results* 152 (eds. A. D. Saunders, H. C. Larsen, S. Wise, and J. R. Allen), pp. 503–533.

Fitton J. G., Larsen L. M., Saunders A. D., Hardarson B. S., and Kempton P. D. (2000) Palaeogene continental to oceanic magmatism on the SE Greenland continental margin at 63 degrees N: a review of the results of ocean drilling program legs 152 and 163. *J. Petrol.* **41**, 951–966.

Francis D., Ludden J., and Hynes A. (1983) Magma evolution in a Proterozoic rifting environment. *J. Petrol.* **24**, 556–582.

Frey F. A., McNaughton N. J., Nelson D. R., deLaeter J. R., and Duncan R. A. (1996) Petrogenesis of the Bunbury Basalt, western Australia: interaction between the Kerguelen plume and Gondwana lithosphere? *Earth Planet. Sci. Lett.* **144**, 163–183.

Frey F. A., Coffin M. F., Wallace P. J., Weis D., Zhao X., Wise S. W., Wahnert V., Teagle D. A. H., Saccocia P. J., Reusch D. N., Pringle M. S., Nicolaysen K. E., Neal C. R., Muller R. D., Moore C. L., Mahoney J. J., Keszthelyi L., Inokuchi H., Duncan R. A., Delius H., Damuth J. E., Damasceno D., Coxall H. K., Borre M. K., Boehm F., Barling J., Arndt N. T., and Antretter M. (2000) Origin and evolution of a submarine large igneous province: the Kerguelen Plateau and Broken Ridge, southern Indian Ocean. *Earth Planet. Sci. Lett.* **176**, 73–89.

Furomoto A. S., Webb J. P., Odegaard M. E., and Hussong D. M. (1976) Seismic studies on the Ontong-Java Plateau, 1970. *Tectonophysics* **34**, 71–90.

Gladczenko T. P., Coffin M. F., and Eldholm O. (1997) Crustal structure of the Ontong Java Plateau: modeling of new gravity and existing seismic data. *J. Geophys. Res.-Solid Earth* **102**, 22711–22729.

Green M. G., Sylvester P. J., and Buick R. (2000) Growth and recycling of early Archaean continental crust: geochemical evidence from the Coonterunah and Warrawoona Groups, Pilbara Craton, Australia. *Tectonophysics* **322**, 69–88.

Griffiths R. W. and Campbell I. H. (1990) Stirring and structure in mantle starting plumes. *Earth Planet. Sci. Lett.* **99**, 66–78.

Hallam A. (1987a) End-Cretaceous mass extinction event: argument for terrestrial causation. *Science* **238**, 1237–1242.

Hallam A. (1987b) Mesozoic marine organic-rich shales. In *Marine Petroleum Source Rocks,* Geological Society of London, Special Publication 26 (eds. J. Brooks and A. J. Fleet), pp. 251–261.

Hallam A. (1989) The case for sea-level change as a dominant causal factor in mass extinction of marine invertebrates. *Phil. Trans. R. Soc. Lond. B* **325**, 437–455.

Hart S. R., Hauri E. H., Oschmann L. A., and Whitehead J. A. (1992) Mantle plumes and entrainment: isotopic evidence. *Science*, **256.**

Hassler D. R. and Shimizu N. (1998) Osmium isotopic evidence for ancient subcontinental lithospheric mantle beneath the Kerguelen Islands, southern Indian Ocean. *Science* **280**, 418–421.

Hauff F., Hoernle K., Tilton G., Graham D. W., and Kerr A. C. (2000a) Large volume recycling of oceanic lithosphere over short time scales: geochemical constraints from the Caribbean Large Igneous Province. *Earth Planet. Sci. Lett.* **174**, 247–263.

Hauff F., Hoernle K., van den Bogaard P., Alvarado G. E., and Garbe-Schonberg C. D. (2000b) Age and geochemistry of basaltic complexes in western Costa Rica: contributions to the geotectonic evolution of Central America. *Geochem. Geophys. Geosys.* **1**, Paper number 1999GC000020.

Hergt J. M. and Brauns C. M. (2001) On the origin of Tasmanian dolerites. *Aust. J. Earth Sci.* **48**, 543–549.

Hill R. I. (1991) Starting plumes and continental break-up. *Earth Planet. Sci. Lett.* **104**, 398–416.

Hollings P. and Wyman D. (1999) Trace element and Sm-Nd systematics of volcanic and intrusive rocks from the 3 Ga Lumby Lake Greenstone belt, Superior Province: evidence for Archean plume-arc interaction. *Lithos* **46**, 189–213.

Holmes A. (1918) The basaltic rocks of the Arctic region. *Min. Mag.* **18**, 180–222.

Hémond C., Arndt N. T., Lichtenstein U., Hofmann A. W., Oskarsson N., and Steinthorsson S. (1993) The heterogeneous Iceland plume: Nd–Sr–O isotopes and trace element constraints. *J. Geophys. Res.* **98**, 15833–15850.

Isozaki Y. (1997) Jurassic accretion tectonics of Japan. *Island Arc* **6**, 25–51.

Jenkyns H. C. (1980) Cretaceous anoxic events: from continents to oceans. *J. Geol. Soc. London* **137**, 171–188.

Jochum K. P., Arndt N. T., and Hofmann A. W. (1991) Nb–Th–La in komatiites and basalts: constraints on komatiite petrogenesis and mantle evolution. *Earth Planet. Sci. Lett.* **107**, 272–289.

Jones G., Sano H., and Valsamijones E. (1993) Nature and Tectonic setting of accreted basalts from the Mino terrane central Japan. *J. Geol. Soc. London* **150**, 1167–1181.

Kaiho K. (1994) Planktonic and benthic foraminiferal extinction events during the last 100 m.y. *Palaeogeog. Palaeoclim. Palaeoecol.* **111**, 45–71.

Kempton P. D., Fitton J. G., Saunders A. D., Nowell G. M., Taylor R. N., Hardarson B. S., and Pearson G. (2000) The Iceland plume in space and time: a Sr–Nd–Pb–Hf study of the North Atlantic rifted margin. *Earth Planet. Sci. Lett.* **177**, 255–271.

Kent R. W., Saunders A. D., Kempton P. D., and Ghose N. C. (1997) Rajmahal basalts, eastern India: mantle sources and melt distribution at a volcanic rifted margin. In *Large*

Igneous Provinces: Continental, Oceanic and Planetary Volcanism, American Geophysical Union Monograph 100 (eds. J. J. Mahoney and M. Coffin), pp. 144–182.

Kerr A. C. (1997) Asteroid impact and mass extinction at the K-T boundary: an extinct red herring? *Geol. Today* **13**, 157–159.

Kerr A. C. (1998) Oceanic plateau formation: a cause of mass extinction and black shale deposition around the Cenomanian–Turonian boundary. *J. Geol. Soc. London* **155**, 619–626.

Kerr A. C., Kempton P. D., and Thompson R. N. (1995a) Crustal assimilation during turbulent magma ascent (ATA): new isotopic evidence from the Mull Tertiary lava succession, NW Scotland. *Contrib. Mineral. Petrol.* **119**, 142–154.

Kerr A. C., Saunders A. D., Tarney J., Berry N. H., and Hards V. L. (1995b) Depleted mantle plume geochemical signatures: no paradox for plume theories. *Geology* **23**, 843–846.

Kerr A. C., Marriner G. F., Arndt N. T., Tarney J., Nivia A., Saunders A. D., and Duncan R. A. (1996a) The petrogenesis of komatiites, picrites and basalts from the Isle of Gorgona, Colombia: new field, petrographic and geochemical constraints. *Lithos* **37**, 245–260.

Kerr A. C., Tarney J., Marriner G. F., Klaver G. T., Saunders A. D., and Thirlwall M. F. (1996b) The geochemistry and petrogenesis of the late-Cretaceous picrites and basalts of Curaçao Netherlands Antilles: a remnant of an oceanic plateau. *Contrib. Mineral. Petrol.* **124**, 29–43.

Kerr A. C., Marriner G. F., Tarney J., Nivia A., Saunders A. D., Thirlwall M. F., and Sinton C. W. (1997a) Cretaceous basaltic terranes in western Colombia: elemental, chronological and Sr–Nd constraints on petrogenesis. *J. Petrol.* **38**, 677–702.

Kerr A. C., Tarney J., Marriner G. F., Nivia A., and Saunders A. D. (1997b) The Caribbean–Colombian Cretaceous igneous province: the internal anatomy of an oceanic plateau. In *Large Igneous Provinces; Continental, Oceanic and Planetary Flood Volcanism,* American Geophysical Union Monograph 100 (eds. J. J. Mahoney and M. Coffin), pp. 45–93.

Kerr A. C., Tarney J., Nivia A., Marriner G. F., and Saunders A. D. (1998) The internal structure of oceanic plateaus: Inferences from obducted Cretaceous terranes in western Colombia and the Caribbean. *Tectonophysics* **292**, 173–188.

Kerr A. C., Iturralde-Vinent M. A., Saunders A. D., Babbs T. L., and Tarney J. (1999) A new plate tectonic model of the Caribbean: implications from a geochemical reconnaissance of Cuban Mesozoic volcanic rocks. *Geol. Soc. Am. Bull.* **111**, 1581–1599.

Kerr A. C., White R. V., and Saunders A. D. (2000) LIP reading: recognizing oceanic plateaux in the geological record. *J. Petrol.* **41**, 1041–1056.

Kerr A. C., Tarney J., Kempton P. D., Spadea P., Nivia A., Marriner G. F., and Duncan R. A. (2002) Pervasive mantle plume head heterogeneity: evidence from the late Cretaceous Caribbean–Colombian Oceanic Plateau. *J. Geophys. Res.* **107**(7), DOI. 10.1029, 2001JB000790.

Kimura G. and Ludden J. (1995) Peeling oceanic crust in subduction zones. *Geology* **23**, 217–220.

Kimura G., Ludden J. N., Desrochers J. P., and Hori R. (1993) A model of ocean-crust accretion for the Superior Province, Canada. *Lithos* **30**, 337–355.

Kimura G., Sakakibara M., and Okamura M. (1994) Plumes in central Panthalassa? deductions from accreted oceanic fragments in Japan. *Tectonics* **13**, 905–916.

Klaver, G. T. (1987) The Curaçao lava formation an ophiolitic analogue of the anomalous thick layer 2B of the mid-Cretaceous oceanic plateaus in the western Pacific and central Caribbean. PhD Thesis, University of Amsterdam, The Netherlands.

Klosko E. R., Russo R. M., Okal E. A., and Richardson W. P. (2001) Evidence for a rheologically strong chemical mantle root beneath the Ontong-Java Plateau. *Earth Planet. Sci. Lett.* **186**, 347–361.

Kroenke L. W. (1974) Origin of continents through development and coalescence of oceanic flood basalt plateaus. *EOS* **55**, 443.

Lahaye Y., Arndt N., Byerly G., Chauvel C., Fourcade S., and Gruau G. (1995) The influence of alteration on the trace-element and Nd isotopic compositions of komatiites. *Chem. Geol.* **126**, 43–64.

Larson R. L. (1991) Geological consequences of super plumes. *Geology* **19**, 963–966.

Lassiter J. C., DePaolo D. J., and Mahoney J. J. (1995) Geochemistry of the Wrangellia flood basalt province: implications for the role of continental and oceanic lithosphere in flood basalt genesis. *J. Petrol.* **36**, 983–1009.

Leary P. N. and Rampino M. R. (1990) A multicausal model of mass extinctions: increase in trace metals in the oceans. In *Extinction Events in Earth History*, *Lecture Notes in Earth Science*, 30 (eds. E. G. Kauffman and O. H. Walliser). Springer, Berlin, pp. 45–55.

Leat P. T., Livermore R. A., Millar I. L., and Pearce J. A. (2000) Magma supply in back-arc spreading centre segment E2 East Scotia Ridge. *J. Petrol.* **41**, 845–866.

Loper D. E. (1983) The dynamical and thermal structure of deep mantle plumes. *Phy. Earth Planet. Int.* **33**, 304–317.

Lucas S. B., Stern R. A., Syme E. C., Reilly B. A., and Thomas D. J. (1996) Intraoceanic tectonics and the development of continental crust: 1.92–1.84 Ga evolution of the Flin Flon belt, Canada. *Geol. Soc. Am. Bull.* **108**, 602–629.

Mahoney J. J., Storey M., Duncan R. A., Spencer K. J., and Pringle M. (1993a) Geochemistry and age of the Ontong Java Plateau. In *The Mesozoic Pacific: Geology, Tectonics, and Volcanism,* American Geophysical Union Monograph 77 (eds. M. S. Pringle, W. W. Sager, W. V. Sliter and S. Stein), pp. 233–261.

Mahoney J. J., Storey M., Duncan R. A., Spencer K. J., and Pringle M. (1993b) Geochemistry and geochronology of Leg 130 basement lavas: nature and origin of the Ontong Java Plateau. In *Proceedings of the Ocean Drilling Program, Scientific Results* 130 (eds. W. H. Berger, L. W. Kroenke, and L. A. Mayer), pp. 3–22.

Mahoney J. J., Jones W. B., Frey F. A., Salters V. J. M., Pyle D. G., and Davies H. L. (1995) Geochemical characteristics of lavas from Broken Ridge, the Naturaliste Plateau and southernmost Kerguelen Plateau: cretaceous plateau volcanism in the Southeast Indian Ocean. *Chem. Geol.* **120**, 315–345.

Mahoney, J. J., Fitton, J. G., Wallace, P. J., *et al*. (2001). *Proceedings of the ODP, Initial Reports.*, 192 [Online]. Available from World Wide Web: <http://www.odp.tamu.edu/publications/192_IR/192ir.htm>. [Cited 2002-02-20].

Marzoli A., Renne P. R., Piccirillo E. M., Ernesto M., Bellieni G., and De Min A. (1999) Extensive 200-million-year-old continental flood basalts of the Central Atlantic Magmatic Province. *Science* **284**, 616–618.

Mauffret A. and Leroy S. (1997) Seismic stratigraphy and structure of the Caribbean igneous province. *Tectonophysics* **283**, 61–104.

McKenzie D. P. and Bickle M. J. (1988) The volume and composition of melt generated by extension of the lithosphere. *J. Petrol.* **29**, 625–679.

McLean D. M. (1985) Deccan traps and mantle degassing in the terminal Cretaceous marine extinctions. *Cret. Res.* **6**, 235–259.

Morgan W. J. (1981) Hotspot tracks and the opening of the Atlantic and Indian Oceans. In *The Oceanic Lithosphere* (ed. C. Emiliani), Wiley-Interscience, pp. 443–487.

Neal C. R., Mahoney J. J., Kroenke L. W., Duncan R. A., and Petterson M. G. (1997) The Ontong Java Plateau. In *Large Igneous Provinces; Continental, Oceanic and Planetary Flood Volcanism,* American Geophysical Union Monograph 100 (eds. J. J. Mahoney and M. Coffin), pp. 183–216.

Nicolaysen K., Bowring S., Frey F., Weis D., Ingle S., Pringle M. S., and Coffin M. F. (2001) Provenance of Proterozoic

garnet-biotite gneiss recovered from Elan Bank Kerguelen Plateau, southern Indian Ocean. *Geology* **29**, 235–238.

Nowell G. M., Kempton P. D., and Noble S. R. (1998) High precision Hf isotope measurements of MORB and OIB by thermal ionisation mass spectrometry: insights into the depleted mantle. *Chem. Geol.* **149**, 211–233.

Operto S. and Charvis P. (1996) Deep structure of the southern Kerguelen Plateau (southern Indian Ocean) from ocean bottom seismometer wide-angle seismic data. *J. Geophys. Res.* **101**, 25077–25103.

Orth C. J., Attrep M., Quintana L. R., Elder W. P., Kauffman E. G., Diner R., and Villamil T. (1993) Elemental abundance anomalies in the late Cenomanian extinction interval: a search for the source(s). *Earth Planet. Sci. Lett.* **117**, 189–204.

Pallister J. S., Budahn J. R., and Murchey B. L. (1989) Pillow basalts of the Angayucham terrane—oceanic plateau and island crust accreted to the Brooks Range. *J. Geophys. Res* **94**, 15901–15923.

Peltonen P., Kontinen A., and Huhma H. (1996) Petrology and geochemistry of metabasalts from the 1.95 Ga Jormua Ophiolite, northeastern Finland. *J. Petrol.* **37**, 1359–1383.

Petterson M. G., Neal C. R., Mahoney J. J., Kroenke L. W., Saunders A. D., Babbs T. L., Duncan R. A., Tolia D., and McGrail B. (1997) Structure and deformation of north and central Malaita, Solomon Islands: tectonic implications for the Ontong Java Plateau—Solomon arc collision, and for the fate of oceanic plateaus. *Tectonophysics* **283**, 1–33.

Petterson M. G., Babbs T., Neal C. R., Mahoney J. J., Saunders A. D., Duncan R. A., Tolia D., Magu R., Qopoto C., Mahoa H., and Natogga D. (1999) Geological-tectonic framework of Solomon Islands, SW Pacific: crustal accretion and growth within an intra-oceanic setting. *Tectonophysics* **301**, 35–60.

Polat A., Kerrich R., and Wyman D. A. (1998) The late Archean Schreiber-Hemlo and White River Dayohessarah greenstone belts, Superior Province: collages of oceanic plateaus, oceanic arcs, and subduction-accretion complexes. *Tectonophysics* **289**, 295–326.

Pringle M. S. (1992) Radiometric ages of basaltic basement recovered at Sites 800, 801, and 802, Leg 129, western Pacific Ocean. In *Proceedings of the Ocean Drilling Program, Scientific Results* 129 (eds. R. L. Larson, Y. Lancelot, A. Fisher and E. L. Winterer). Ocean Drilling Program, Texas A&M University, pp. 389–404.

Puchtel I. S. and Zhuravlev D. Z. (1993) Petrology of mafic-ultramafic metavolcanics and related rocks from the Olondo greenstone belt, Aldan Shield. *Petrol.* **1**, 308–348.

Puchtel I. S., Haase K. M., Hofmann A. W., Chauvel C., Kulikov V. S., Garbe Schonberg C. D., and Nemchin A. A. (1997) Petrology and geochemistry of crustally contaminated komatiitic basalts from the Vetreny Belt, southeastern Baltic Shield: evidence for an early Proterozoic mantle plume beneath rifted Archean continental lithosphere. *Geochim. Cosmochim. Acta* **61**, 1205–1222.

Puchtel I. S., Arndt N. T., Hofmann A. W., Haase K. M., Kroner A., Kulikov V. S., Kulikova V. V., Garbe Schonberg C. D., and Nemchin A. A (1998a) Petrology of mafic lavas within the Onega plateau, central Karelia: evidence for 2.0 Ga plume-related continental crustal growth in the Baltic Shield. Contrib. Miner. *Petrol.* **130**, 134–153.

Puchtel I. S., Hofmann A. W., Mezger K., Jochum K. P., Shchipansky A. A., and Samsonov A. V. (1998b) Oceanic plateau model for continental crustal growth in the archaean, a case study from the Kostomuksha greenstone belt, NW Baltic Shield. *Earth Planet. Sci. Lett.* **155**, 57–74.

Puchtel I. S., Hofmann A. W., Amelin Y. V., Garbe-Schonberg C. D., Samsonov A. V., and Schipansky A. A. (1999) Combined mantle plume-island arc model for the formation of the 2.9 Ga Sumozero-Kenozero greenstone belt, SE Baltic Shield: isotope and trace element constraints. *Geochim. Cosmochim. Acta* **63**, 3579–3595.

Renne P. R. and Basu A. R. (1991) Rapid eruption of the Siberian traps flood basalts at the Permo-Triassic boundary. *Science* **253**, 175–178.

Revillon S., Arndt N. T., Hallot E., Kerr A. C., and Tarney J. (1999) Petrogenesis of picrites from the Caribbean Plateau and the North Atlantic magmatic province. *Lithos* **49**, 1–21.

Reynaud C., Jaillard E., Lapierre H., Mamberti M., and Mascle G. H. (1999) Oceanic plateau and island arcs of southwestern Ecuador: their place in the geodynamic evolution of northwestern South America. *Tectonophysics* **307**, 235–254.

Richards M. A., Duncan R. A., and Courtillot V. E. (1989) Flood basalts and hot spot tracks: plume heads and tails. *Science* **246**, 103–107.

Richards M. A., Jones D. L., Duncan R. A., and DePaolo D. J. (1991) A mantle plume initiation model for the formation of Wrangellia and other oceanic flood basalt plateaus. *Science* **254**, 263–267.

Riley T. R. and Knight K. B. (2001) Age of pre-break-up Gondwana magmatism. *Antar. Sci.* **13**, 99–110.

Royer J.-Y. and Coffin M. F. (1992) Jurassic to Eocene plate tectonic reconstructions in the Kerguelen Plateau region. In *Proceedings of the Ocean Drilling Program, Scientific Results*, 120 (eds. J. S. W. Wise, A. P. Julson, R. Schlich, and E. Thomas), Ocean Drilling Program, Texas A&M University, pp. 917–930 .

Salters V. J. M. (1996) The generation of mid-ocean ridge basalts from the Hf and Nd isotope perspective. *Earth Planet. Sci. Lett.* **141**, 109–123.

Salters V. J. M. and Hart S. R. (1991) The mantle sources of ocean ridges, islands and arcs: the Hf-isotope connection. *Earth Planet. Sci. Lett.* **104**, 364–380.

Salters V. J. M., Storey M., Sevigny J. H., and Whitechurch H. (1992) Trace element and isotopic characteristics of Kerguelen-Heard Plateau basalts. In *Proceedings of the Ocean Drilling Program, Scientific Results* (eds. J. S. W. Wise, A. P. Julson, R. Schlich, and E. Thomas). Ocean Drilling Program, Texas A&M University, vol. 120, pp. 55–62. .

Saunders A. D., Storey M., Kent R. W., and Norry M. J. (1992) Consequences of plume-lithosphere interactions. In *Magmatism and the Causes of Continental Breakup* (eds. B. C. Storey, T. Alabaster, and R. J. Pankhurst). Geological Society of London, London, vol. 68, pp. 41–60.

Saunders A. D., Tarney J., Kerr A. C., and Kent R. W. (1996) The formation and fate of large igneous provinces. *Lithos* **37**, 81–95.

Saunders A. D., Fitton J., Kerr A. C., Norry M. J., and Kent R. W. (1997) The North Atlantic Igneous Province. In *Large Igneous Provinces: Continental, Oceanic and Planetary Volcanism,* American Geophysical Union Monograph 100 (eds. J. J. Mahoney and M. Coffin), pp. 45–93.

Schlanger S. O., Arthur M. A., Jenkyns H. C., and Scholle P. A. (1987) The Cenomanian–Turonian oceanic anoxic events: I. Stratigraphy and distribution of organic carbon-rich beds and the marine ^{13}C excursion. In *Marine Petroleum Source Rocks,* Geological Society of London, Special Publication 26 (eds. J. Brooks and A. J. Fleet), pp. 371–399.

Sepkoski J. J. (1986) Phanerozoic overview of mass extinction. In *Pattern and Processes in the History of Life* (eds. D. Raup and D. Japlonski). Springer-Verlag, pp. 277–295.

Sinton C. W. and Duncan R. A. (1997) Potential links beween ocean plateau volcanism and global ocean anoxia at the Cenomanian–Turonian boundary. *Econ. Geol.* **92**, 836–842.

Sinton C. W., Duncan R. A., Storey M., Lewis J., and Estrada J. J. (1998) An oceanic flood basalt province within the Caribbean plate. *Earth Planet. Sci. Lett.* **155**, 221–235.

Sinton C. W., Sigurdsson H., and Duncan R. A. (2000) Geochronology and petrology of the igneous basement at the lower Nicaraguan Rise, Site 1001 In *Proceedings of the Ocean Drilling Program, Scientific Results* 165

(ed. P. Garman). Texas A & M University, Ocean Drilling Program, College Station, TX, United States, pp. 233–236.

Skulski T. and Percival J. A. (1996) Allochthonous 2.78 Ga oceanic plateau slivers in a 2.72 Ga continental arc sequence: vizien greenstone belt, northeastern Superior Province, Canada. *Lithos*, **37**, 163–179.

Smith H. S. and Erlank A. J. (1982) Geochemistry and petrogenesis of komatiites from the Barberton greenstone belt. In *Komatiites* (eds. N. T. Arndt and E. G. Nisbet). Allen and Unwin, pp. 347–398.

Stein M. and Goldstein S. L. (1996) From plume head to continental lithosphere in the Arabian-Nubian shield. *Nature* **382**, 773–778.

Stein M. and Hofmann A. W. (1994) Mantle plumes and episodic crustal growth. *Nature* **372**, 63–68.

Stern R. A., Syme E. C., and Lucas S. B. (1995) Geochemistry of 1.9 Ga MORB- and OIB-like basalts from the Amisk collage, Flin Flon Belt, Canada: evidence for an intra-oceanic origin. *Geochim. Cosmochim. Acta* **59**, 3131–3154.

Storey M., Saunders A. D., Tarney J., Gibson I. L., Norry M. J., Thirlwall M. F., Leat P., Thompson R. N., and Menzies M. A. (1989) Contamination of Indian Ocean asthenosphere by the Kerguelen-Heard mantle plume. *Nature* **338**, 574–576.

Storey M., Mahoney J. J., Kroenke L. W., and Saunders A. D. (1991) Are oceanic plateaus sites of komatiite formation? *Geology* **19**, 376–379.

Storey M., Mahoney J. J., Saunders A. D., Duncan R. A., Kelley S. P., and Coffin M. F. (1995) Timing of hot spot-related volcanism and the breakup of Madagascar and India. *Science* **267**, 852–855.

Sun S.-S. and McDonough W. F. (1989) Chemical and isotope systematics of oceanic basalts: implications for mantle composition and processes. in *Magmatism in the Ocean Basins,* Geological Society of London, Special Publication 42 (eds. A. D. Saunders and M. J. Norry), pp. 313–345.

Tardy M., Lapierre H., Struik L. C., Bosch D., and Brunet P. (2001) The influence of mantle plume in the genesis of the Cache Creek oceanic igneous rocks: implications for the geodynamic evolution of the inner accreted terranes of the Canadian Cordillera. *Can. J. Earth Sci.* **38**, 515–534.

Tatsumi Y., Shinjoe H., Ishizuka H., Sager W. W., and Klaus A. (1998) Geochemical evidence for a mid-Cretaceous superplume. *Geology* **26**, 151–154.

Tatsumi Y., Kani T., Ishizuka H., Maruyama S., and Nishimura Y. (2000) Activation of Pacific mantle plumes during the Carboniferous: evidence from accretionary complexes in southwest Japan. *Geology* **28**, 580–582.

Tejada M. L. G., Mahoney J. J., Duncan R. A., and Hawkins M. P. (1996) Age and geochemistry of basement and alkalic rocks of Maliata and Santa Isabel, Solomon Islands, southern margin of Ontong Java Plateau. *J. Petrol.* **37**, 361–394.

Tejada M. L. G., Mahoney J. J., Neal C. R., Duncan R. A., and Petterson M. G. (2002) Basement geochemistry and geochronology of Central Malaita, Solomon Islands, with implications for the origin and evolution of the Ontong Java Plateau. *J. Petrol.* **43**, 449–484.

Thirlwall M. F., Graham A. M., Arculus R. J., Harmon R. S., and Macpherson C. G. (1996) Resolution of the effects of crustal assimilation, sediment subduction and fluid transport in island arc magmas: Pb–Sr–Nd–O isotope geochemistry of Grenada, Lesser Antilles. *Geochim. Cosmochim. Acta* **60**, 4785–4810.

Thompson R. N., Dickin A. P., Gibson I. L., and Morrison M. A. (1982) Elemental fingerprints of isotopic contamination of Hebridean Palaeocene mantle-derived magmas by Archaean sial. *Contrib. Mineral. Petrol.* **79**, 159–168.

Thompson P. M. E., Kempton P. D., White R. V., Kerr A. C., Tarney J., Saunders A. D., and Fitton J. G. (2004) Hf-Nd isotope constraints on the origin of the Cretaceous Caribbean plateau and its relationship to the Galapagos plume. *Earth Planet. Sci. Lett.* (in press).

Tomlinson K. Y., Stevenson R. K., Hughes D. J., Hall R. P., Thurston P. C., and Henry P. (1998) The Red Lake greenstone belt, Superior Province: evidence of plume-related magmatism at 3 Ga and evidence of an older enriched source. *Precamb. Res.* **89**, 59–76.

Tomlinson K. Y., Hughes D. J., Thurston P. C., and Hall R. P. (1999) Plume magmatism and crustal growth at 2.9 to 3.0 Ga in the Steep Rock and Lumby Lake area, Western Superior Province. *Lithos* **46**, 103–136.

Viereck L. G., Taylor P. N., Parson L. M., Morton A. C., Hertogen J., Gibson I. L., and Party O. S. (1988) Origin of the Palaeogene Vøring Plateau volcanic sequence. In *Early Tertiary Volcanism and the Opening of the NE Atlantic,* Geological Society London Special Publication 39 (eds. A. C. Morton and L. M. Parson), pp. 69–83.

Vogt P. R. (1989) Volcaniogenic upwelling of anoxic, nutrient-rich water: a possible factor in carbonate-bank/reef demise and benthic faunal extinctions. *Bull. Geol. Soc. Amer.* **101**, 1225–1245.

Walker R. J., Storey M. J., Kerr A. C., Tarney J., and Arndt N. T. (1999) Implications of 1870s isotopic heterogeneities in a mantle plume: evidence from Gorgona Island and Curaçao. *Geochim. Cosmochim. Acta* **63**, 713–728.

Weis D. and Frey F. A. (1996) Role of the Kerguelen Plume in generating the eastern Indian Ocean seafloor. *J. Geophy. Res.* **101**, 13831–13849.

White R. S. and McKenzie D. P. (1989) Magmatism at rift zones: the generation of volcanic continental margins. *J. Geophy. Res.* **94**, 7685–7729.

White R. V., Tarney J., Kerr A. C., Saunders A. D., Kempton P. D., Pringle M. S., and Klaver G. T. (1999) Modification of an oceanic plateau, Aruba, Dutch Caribbean: implications for the generation of continental crust. *Lithos* **46**, 43–68.

Wilde P., Quinby-Hunt M. S., and Berry B. N. (1990) Vertical advection from oxic or anoxic water from the pycnocline as a cause of rapid extinction or rapid radiations. In *Extinction Events in Earth History. Lecture Notes in Earth Science* (eds. E. G. Kauffman and O. H. Walliser). Springer, vol. 30, pp. 85–97.

Wilson J. T. (1963) A possible origin of the Hawaiian Islands. *Can. J. Phy.* **41**, 863–870.

Wood D. A., Mattey D. P., Joron J. L., Marsh N. G., Tarney J., and Treuil M. (1980) A geochemical study of 17 selected samples from basement cores recovered at Sites 447, 448, 449, 450, and 453, Deep Sea Drilling Project Leg 59. In *Initial Reports of the Deep Sea Drilling Project* 59 (eds. L. Kroenke, R. Scott, and *et al.*) U.S. Government Printing Office, pp. 743–752.

Woodhead J. D., Eggins S. M., and Johnson R. W. (1998) Magma genesis in the New Britain island arc: further insights into melting and mass transfer processes. *J. Petrol.* **39**, 1641–1668.

Zindler A. and Hart S. R. (1986) Chemical geodynamics. *Ann. Rev. Earth Planet. Sci.* **14**, 493–571.

Treatise On Geochemistry
ISBN (set): 0-08-043751-6
Volume 3; (ISBN: 0-08-044338-9); pp. 537–565